

## Evaluation of Variation in Source Parameters of Repeating Characteristic Subduction Earthquakes in Case of Characteristic Earthquakes off Kesenuma, northeast Japan

\*KimiYuki Asano<sup>1</sup>

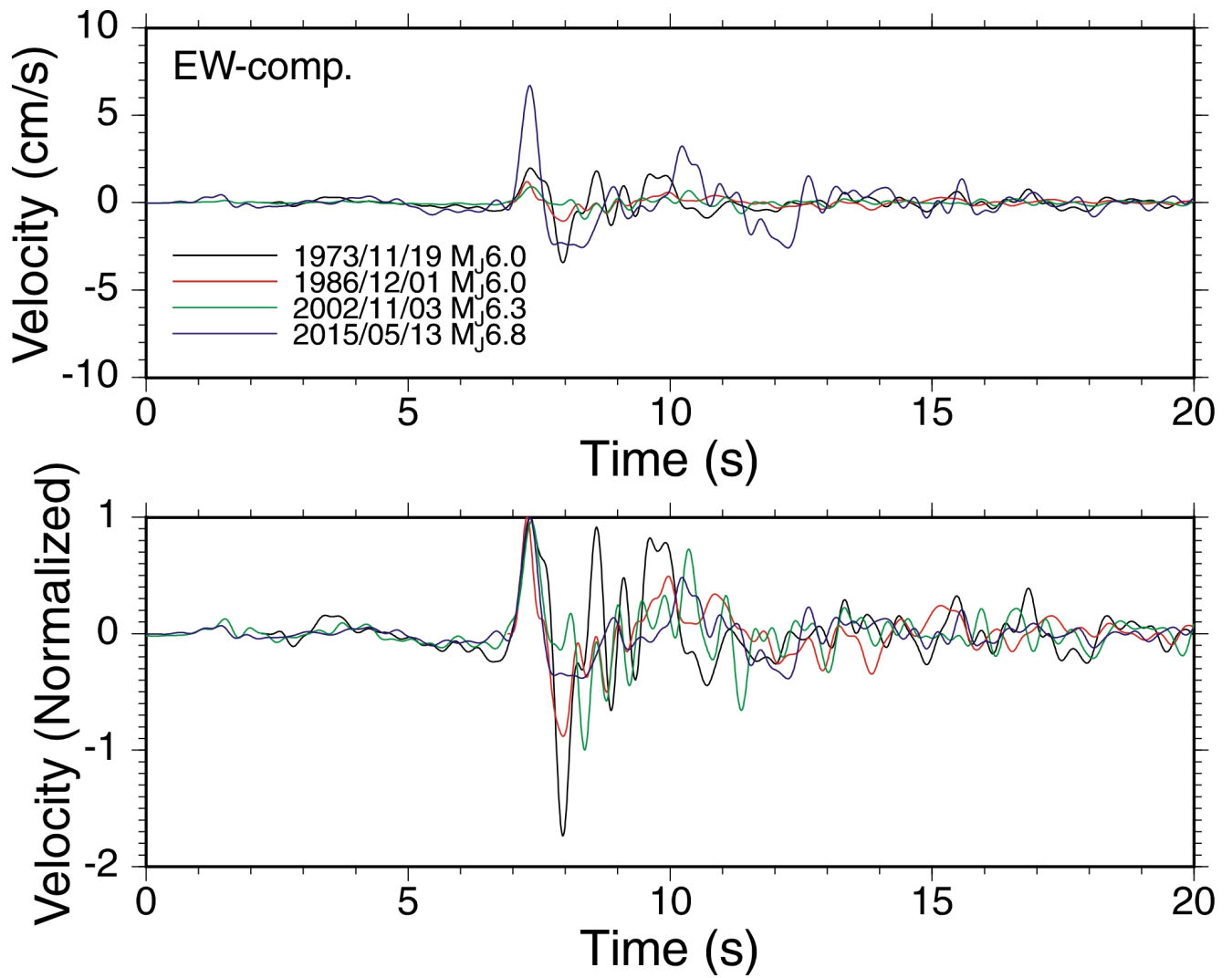
1. Disaster Prevention Research Institute, Kyoto University

After the experience of the 2011 Tohoku earthquake, scenario-based strong motion prediction is strongly required quantitatively to show its variation or uncertainty. In this presentation, we focus on the variation or uncertainty of source parameters such as area and stress drop of strong motion generation area (SMGA). In the strong motion prediction recipe, outer and inner source parameters are given by the empirical scaling relationships (e.g., Murotani *et al.*, 2008). Each empirical scaling relationship has its standard deviation. However, such standard deviation is combination of variation due to difference in source characteristics among many different source regions and one due to the deviation among repeating events in a specific source region. In order to develop more sophisticated strong motion prediction, we would like to separate these two factors of variations from each other to obtain reasonable probabilistic distributions of source parameters by analyzing repeating characteristic earthquakes occurring in a same source region. Nagai *et al.* (2001) and Yamanaka and Kikuchi (2004) are pioneering studies for such objectives, however, what aspect of SMGA will be preserved and deviated is need to be investigated for advancing strong motion prediction framework. Particularly in northeast Japan, repeating characteristic subduction earthquakes have been observed during the history of strong motion observation. For example, Takiguchi *et al.* (2011) analyzed SMGAs for the 1982 and 2008 off Ibaraki earthquakes (both events are  $M_{j}7.0$ ), and they concluded that the size of SMGA is same for two events, but the stress drop of SMGA for the 1982 event is 1.5 times larger than that of 2008 event.

In this study, repeating characteristic subduction earthquakes occurring off Kesenuma, northeast Japan, are analyzed. The latest event occurred on May 13, 2015 ( $M_{j}6.8$ ). According to Hasegawa *et al.* (2005) and Takasai *et al.* (2014),  $M_6$ -class events repeatedly occurred in 1940, 1954, 1973, 1986, and 2002. They showed that the average repeating period is 15.5 years and the average JMA magnitude is 6.3. Two events occurring in 2002 and 2015 are densely observed by K-NET and KiK-net operated by NIED. PARI continues strong motion observation in many ports over 50 years, and four events (1974, 1986, 2002, and 2015) were observed by their network. The figure below shows comparison of the EW components of observed velocities in 0.2–2 Hz at Ofunato-Bochi station of PARI. The pulse length of the direct S-wave is almost same for these four events, but the maximum amplitude of the 2015 event is largest among the four events. From above comparison, the size of SMGA for these four events might be almost equivalent to each other, and the difference in the waveforms reflects the difference in stress drop of SMGA. We will further discuss on the variation in stress drop based on the spectral ratio method and waveform modeling.

Acknowledgements: The strong motion data from K-NET, KiK-net (NIED) and PARI are used in this study.

Keywords: Repeating characteristic earthquakes, Source characteristics, Strong motion generation area



## A study on effects of uncertainty in fault width to strong motion evaluation for earthquakes in active faults

\*Nobuyuki Morikawa<sup>1</sup>, Takahiro Maeda<sup>1</sup>, Asako Iwaki<sup>1</sup>, Hiroyuki Fujiwara<sup>1</sup>

1.National Research Institute for Earth Science and Disaster Prevention

The lower-depth of the seismogenic zone is estimated from hypocenter distribution of small earthquakes in the long-term evaluation of earthquakes in active faults by Earthquake Research Committee of Japan (ERCJ), but there is a possibility that the fault bottom becomes deeper than that when a large earthquake occurs. However, almost no knowledge how deep it is. Therefore the consideration of epistemic uncertainty in the lower-depth of the seismogenic zone, the fault width, is required in the strong-motion evaluation.

The magnitude of an earthquake changes with the fault width by using the method (A) of strong motion evaluation method "recipe" by ERCJ. On the other hand, the magnitude of an earthquake is determined from the fault length by using the method (B) of the "recipe". Therefore the magnitude of an earthquake does not change with the fault width, but the values of source parameters, such as slip and static stress drop, change because the relation between seismic moment and fault area vary in this case.

As mentioned above, dependence of fault width on outer- and inner-source parameters determined from the "recipe" is very complicated. In this study we examine calculations of strong ground motion for some models considering uncertainty of the lower depth of the seismogenic zone and compare the results. It is also necessary to consider the uncertainty in dip angle of the fault as the parameter related to the fault width, but we consider only uncertainty in the lower-depth of the seismogenic zone here.

Keywords: Uncertainty, Strong ground motion, Fault width, Active faults

## Construction of a recipe for predicting strong ground motions from subduction mega-thrust earthquakes

\*Kojiro Irikura<sup>1</sup>, Susumu Kurahashi<sup>1</sup>

1.Aichi Institute of Technology

### Introduction

Before the 2011 Mw 9 Tohoku earthquake, there are considered six segments for the region off the coast of Tohoku from Middle Sanriku-Oki to Ibaragi-Oki with seismic activities of past 400 years by the Headquarter of Earthquake Research Promotion, Japan (HERP). Then, they made a long-term forecast that Mw 7-8.4 earthquakes would occur within those segments, having different recurrence times from one to the other. Prior to the Mw 9 event, the possibility of a megathrust earthquake of magnitude larger than 8.5 was never expected from a scientific point of view. On the other hand, we find the segmentation might control the characteristics of ground motions from the rupture process inversion of near-field strong motion records as well as earthquake occurrence in the source region of this event. Then, we propose an improved idea for recipe of predicting strong ground motions for subduction earthquakes.

### Segmentation

There were not only along-strike segments but also along-dip ones for the source region of the Mw 9 event. The high frequency radiation is dominated from SMGAs in segments located in a down-dip region closer to Japan coast similar to high-frequency backprojection studies using teleseismic short-period P waves data. The low frequency radiation from the asperity inverted from long-period strong-motions data tends to dominate in the shallow segment closer to the trench. Similarly, apparent along-dip rupture differences were observed for several other large megathrust events such as the 2010 Mw 8.8 Maule earthquake in Chile, the 2005 Mw 8.6 Sumatra earthquake, and the 2004 Mw 9.2 Sumatra earthquake by comparing the slip distribution with HF radiation observations (Yao et al., 2015).

### Short-period Source model

From the observed strong motions during the Tohoku event, there are recognized distinctive five wavepackets that correspond to ground motions from respective small asperities. The origins of the wavepackets were retrieved from data arrays consisting of the strong motion stations using a semblance analysis. Then, we estimate a short-period source model for generating strong ground motions from this earthquake by comparing the observed records from the mainshock with synthesized motions based on a multiple-asperity source model and the empirical Green's function method. We find that five small-asperities in the down-dip areas generate short-period motions of engineering interest but large asperities in the shallower area east of hypocenter generate mainly large slip and long-period ground motions. We call such small asperity strong-motion generation area (SMGA). This model provides broadband ground motions including long-period motions from 2 s to 10 s that are engineering interest for aseismic design and base-isolation.

### Impulsive waves from SMGA

Another problem is that the short-period source models with such SMGAs cannot simulate impulsive waves with high acceleration and velocity seen at onsets of the wave-packets in strong motion records observed near the source fault. To generate such impulsive waves, multi-scale source model is needed with heterogeneity of maximum slip velocity and rise time inside the SMGAs. Then the recipe of predicting broadband ground motions from 0.1 s to 10 s for mega-thrust subduction earthquakes is needed to consider the multi-scale heterogeneous model.

Keywords: subduction mega-thrust earthquakes, strong ground motions, short-period source model,  
strong motion prediction recipe

## Near-field strong motion on the hanging wall of low angle thrusting: a case of Hamaoka

\*Ichiro Kawasaki<sup>1</sup>

1.Tono Research Institute of Earthquake Science, Association for the Development of Earthquake Prediction

(1) We discuss the near-field strong motion at Hamaoka on hanging wall of low angle thrusting. The key parameter is slip velocity.

(2) The high stress drop of 22 MPa has raised a problem on the evaluation of near-field strong motion. As far as ever documented in Japan, stress drops of subduction zone earthquakes and average slip velocities were estimated to be around 3-5 MPa and 1 m/s, respectively. Following Starr (1928) for dip slip faulting, a stress drop  $\Delta\sigma$  is proportional to  $D_0/W$ , where  $D_0$  is an average slip and  $W$  is a fault width. Following Brune (1970) and Ida and Aki (1972), an average slip velocity  $D_0/t_0$  is proportional to earthquake generating stress  $\sigma_e$ , where  $t_0$  is a risetime. Assuming that  $\sigma_e$  is the same as  $\Delta\sigma$ , both  $D_0$  and  $D_0/t_0$  are proportional to  $\sigma_e$ , leading to the recognition that velocity and acceleration amplitude of synthetic strong motion are proportional to  $\sigma_e$  in the near-field to the first order.

(3) We move to a discussion of strong motion at Hamaoka. Assuming fault parameters as a fault length 100 km,  $W$  50 km, and bilateral propagation in strike-parallel direction and unilateral propagation upward of rupture front from the center of the lower side, we obtain synthetic strong motion (Fig.1) at Hamaoka for three cases of  $D_0/t_0$  of 1 m/s, 3 m/s and 5 m/s with a common  $D_0$  of 15 m. Numerical computation is done by programs of Kawasaki et al. (1973) and Okada (1980). Velocity and acceleration are roughly proportional to  $D_0/t_0$ . When  $D_0/t_0$  is larger than 3 m/s, the maximum amplitude of acceleration is larger than  $g$ .

(4) We can not apply above discussion to shorter period strong motion because far-field term gets relatively predominant and physical attenuation and scattering become effective. However, on the following assumptions (a) and (b)

(a) velocity and acceleration of strong motion are proportional to slip velocity and earthquake generating stress in every scales of multi-scale rupturing phenomena,

(b) stress level of level 2 megathrust earthquake would be far higher than those of level 1 subduction zone earthquakes,

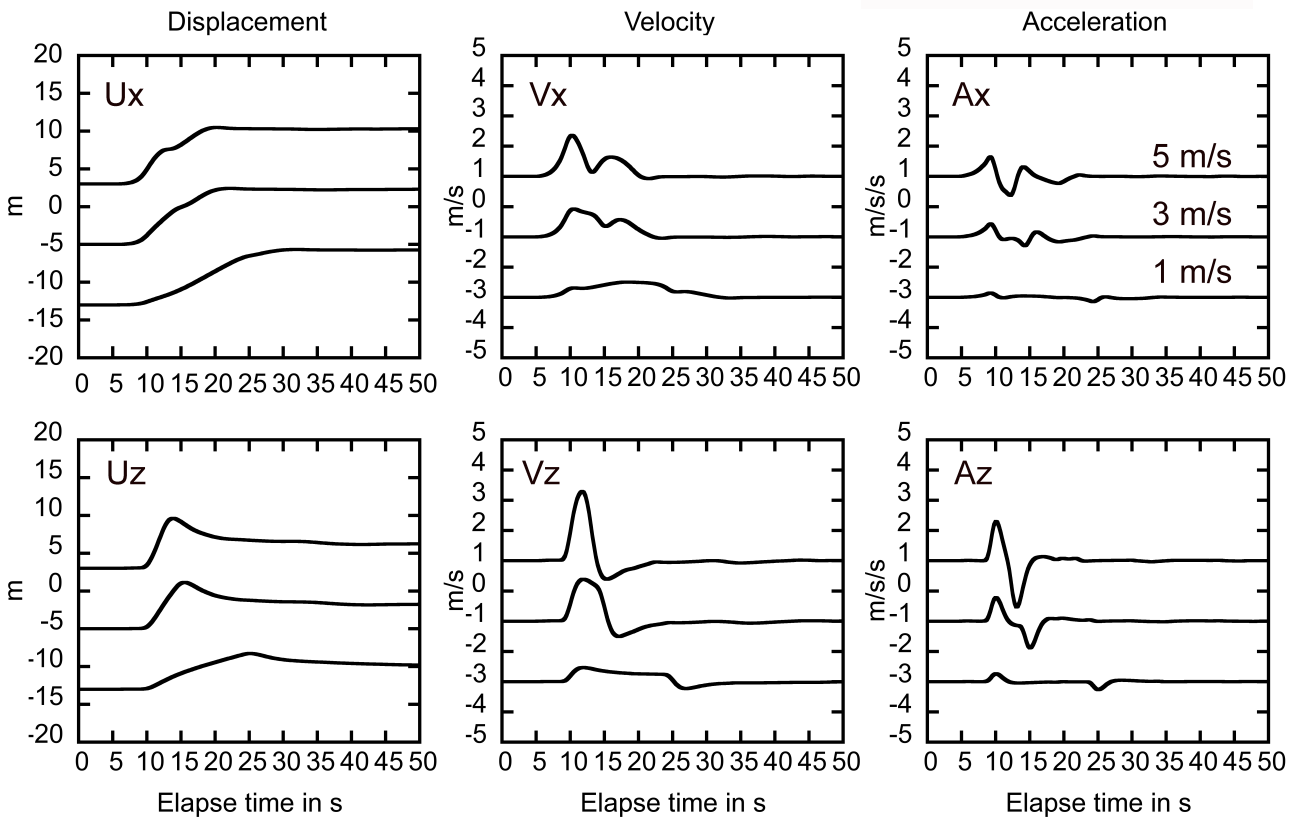
we can postulate that strong motions at Hamaoka during the coming level 2 class Mw9 Nankai trough earthquake would be far larger than those during level 1 class 1944 Tonankai and 1854 Ansei-Tokai earthquakes.

(5) Thus, reliable evaluation of near-field strong motion on the hanging wall of low angle thrusting seems to be not feasible at the present stage of seismology. The evaluation of regional tectonic stress on the hanging wall and the distribution of the strong asperity on the subduction interface are indispensable.

(6) Figure caption

Fig.1 Synthetic strong motions at Hamaoka for three cases of slip velocities of 1 m/s, 3 m/s and 5 m/s with a common slip  $D_0$  of 15 m. Other fault parameters are given in the text. Left, middle and right panels are displacement ( $U$ ), velocity ( $V$ ) and acceleration ( $A$ ), respectively. Upper and lower row panels are those of fault perpendicular motion (subscript  $x$ ) and vertical motion ( $z$ ), respectively. A distance from Hamaoka to subduction interface is 10 km.

Keywords: near-field, low angle thrusting, earthquake generating stress, slip velocity, strong motion, Hamaoka



## Long-period ground motion evaluation for the Sagami Trough megathrust earthquakes

\*Takahiro Maeda<sup>1</sup>, Asako Iwaki<sup>1</sup>, Nobuyuki Morikawa<sup>1</sup>, Ryuta Imai<sup>2</sup>, Shin Aoi<sup>1</sup>, Hiroyuki Fujiwara<sup>1</sup>

1.National Research Institute for Earth Science and Disaster Prevention, 2.Mizuho Information & Research Institute, Inc.

We evaluate long-period ground motions associated with the Sagami Trough earthquakes, especially for the 1703 Genroku earthquake and the 1923 Taisho earthquake. The long-period ground motions are simulated by the finite difference method using a characterized source model and the 3-D velocity structure model. The parameters of the characterized source model are determined based on a "recipe" for predicting strong ground motion [Earthquake Research Committee (ERC), 2009]. We construct 408 source models for hypothetical Genroku and Taisho earthquakes assuming possible source parameters, including asperity configuration, asperity size and hypocenter location (120 models and 288 models for hypothetical Taisho and Genroku earthquakes, respectively). And then we introduce a multi-scale heterogeneity (Sekiguchi and Yoshimi, 2006) of rupture propagation (rupture velocity, slip, rake angle) to the characterized source models. The 3-D velocity structure model used in the simulation is a recently constructing model for the Kanto area (Senna et al., 2015, SSJ). Using these models, an analyzing period range of our simulation is  $>2$  s.

We use peak ground velocity (PGV) and velocity response spectra (Sv) as indices for the evaluation. Spatial distribution maps of PGV and Sv indicate that the hypocenter location has larger impact on the distribution. Because the source areas are located beneath the Kanto plane, body waves predominate in simulated waveforms for station in the plane. Histograms of PGV and Sv show a log-normal like distribution. Using these results, we evaluate the long-period ground motion hazard for two types of Kanto earthquake.

This study was supported by the Support Program for Long-Period Ground Motion Hazard Maps by the Ministry of Education, Culture, Sports, Science and Technology (MEXT).

Keywords: Sagami Trough, Long-period ground motion, Finite difference method

The long-period ground motion between P and S arrivals observed by the deep borehole strainmeters and stressmeters

\*Osamu Murakami<sup>1</sup>, Hiroshi Ishii<sup>1</sup>, Yasuhiro Asai<sup>1</sup>

1.Tono Research Institute of Earthquake Science, Association for the Development of Earthquake Prediction

We deployed multi-component borehole instruments equipped with strainmeters and/or stressmeters around the Tono Research Institute of Earthquake Science (TRIES). We recorded the continuous data at a rate of 1-50 Hz for these instruments. In these records, we observed the long-period variations between P and S arrivals from large earthquakes. In order to investigate the nature of these long-period variations, we estimated the dominant periods of these variations. After we manually picked the P and S wave arrivals for each waveform, we calculated spectrum of the records between P and S wave arrivals. We found that the dominant periods of these long-period variations are typically a few tens seconds. Though W phase (Kanamori, 1993) is well known as the long-period phase between P and S arrivals, the periods of W phase are usually hundreds seconds or more, and are longer than our observed dominant periods. We consider that the observed long-period variations are responsible for other effects, such as PL wave caused by the leaking mode (Yoshii, 1970). These long-periods variations are also recorded by seismometers equipped with the same borehole instruments installed in deep borehole. The long-periods variations observed at seismometers, however, will be clearly found, after we applied the bandpass (0.01 -0.1 Hz) filter. Because the strainmeters and stressmeters have enough sensitivity to DC, we consider that the strainmeters and stressmeters are also useful to detect the long-period ground motions. We will present the results obtained from the analysis.

Keywords: long-period ground motion between P and S arrivals, strainmeters, stressmeters, borehole

## Studying the effect of seawater on seafloor strong ground motions using simulation method

\*Hongqi Diao<sup>1,2</sup>, Jinjun Hu<sup>2</sup>, Lili Xie<sup>2,3</sup>

1.Earthquake Research Institute, The University of Tokyo, Tokyo 113-0032, Japan, 2.Key Laboratory of Earthquake Engineering and Engineering Vibration, Institute of Engineering Mechanics, China Earthquake Administration, Harbin 150080, China, 3.School of Civil Engineering and Architecture, Harbin Institute of Technology, Harbin 150090, China

For the seismic design of offshore engineering, we need to estimate the design parameters of seafloor strong motion. Under the influence of seawater and seafloor soil, seafloor ground motion may present different characteristic from that of onshore ground motion. Until now, there have been very few researches on the seafloor strong motion and also very little seafloor strong motion data has been observed. Our present paper focuses on the effect of seawater on the engineering characteristics and attenuation characteristic of seafloor strong motion. Our main work includes two main parts: one is the effect on engineering characteristics (PGA, Fourier spectra and acceleration response spectra, and 90% energy duration)of seafloor strong motion under seawater of different depth; and the other is the effect of seawater for 50-meter depth on seafloor strong motion attenuation characteristic. Using the wavenumber integration method program of Computer Programs in Seismology (CPS), we perform numerical simulation of seafloor ground motions in six different conditions(water depth: 50 meter, 60 meter, 70 meter, 80 meter, 90 meter and 100 meter) for three kinds of fault types(Normal fault, Reverse fault and Strike-slip fault) and compare them with that without seawater on them. As a result, for whatever kind of fault types, the difference of effect on seafloor horizontal ground motions of seawater is little and can be ignored. However, the effect on seafloor vertical ground motions of seawater is obvious. For all the three kinds of fault types, with the increasing depth of seawater, the effects on vertical motions are similar: 1) waveform becomes more visually complicated; 2) PGA becomes smaller; 3) Fourier spectra decreases greatly near the P wave resonance frequencies of seawater, acceleration response spectra becomes smaller in short periods less than 0.1s. The effect on 90% energy duration time of seafloor vertical motion of seawater has something to do with fault types. We establish the attenuation characteristic relationships of PGA and acceleration response spectra for seafloor vertical ground motion with 50-meter depth of seawater using CPS software and compare them with that without seawater. We found that: the 50-meter depth of seawater has a great effect on the attenuation relationships of PGA and the acceleration response spectra in very short periods (not exceeding 0.04s), the PGA and acceleration response spectra values of seafloor vertical motion are obviously smaller than those without water.

Keywords: seawater, seafloor ground motion, numerical simulation, attenuation characteristic relationship

## Finite Source Modeling of a Large Earthquake Using the Ambient Seismic Field

\*Loic Viens<sup>1</sup>, Hiroe Miyake<sup>2,1</sup>, Kazuki Koketsu<sup>1</sup>

1.Earthquake Research Institute, University of Tokyo, 2.Center for Integrated Disaster Information Research, Interfaculty Initiative in Information Studies, University of Tokyo, Tokyo, Japan

Large ( $M_w \geq 7$ ) earthquakes have the potential to generate long-period seismic waves that can be significantly amplified, even at large distances, by sedimentary basins. Prediction of these long-period ground motions ( $\geq 4$  s) is essential to mitigate their impact on large-scale structures, such as high-rise buildings and oil storage tanks. We focus on the well-recorded Iwate-Miyagi Nairiku earthquake ( $M_w$  6.9), which occurred on 14 June 2008 in the Tohoku region, Japan. This earthquake, which has a reverse-fault mechanism, caused several fatalities, collapse of houses and a bridge, and severe landslides. To simulate the long-period ground motions (4-10 s) generated by this event, we take advantage of the ambient seismic field continuously recorded by seismic stations of the Hi-net/NIED, Japan Meteorological Agency, and Tohoku University networks. Stations located in the vicinity of the mainshock fault plane are used as virtual sources and other stations as receivers. We use the deconvolution method to extract single force impulse response functions between each pair of stations. We first show that, after calibration of the amplitude, impulse response functions accurately simulate the long-period ground motions of a moderate  $M_w$  5.0 aftershock that occurred close to the mainshock hypocenter. To simulate the mainshock, we construct a simple finite source model that is similar to the ones determined by source inversions. The fault plane is first discretized into subfaults of the size of the moderate  $M_w$  5.0 earthquake. We show that it is possible to interpolate the impulse response functions extracted between every virtual source and each receiver to obtain one impulse response function for each subfault. We finally initiate and spread the rupture radially from the hypocenter with a constant velocity to simulate the long-period ground motions. We find that the simulated long-period ground motions are consistent with the earthquake records, which confirm the power of this technique to assess seismic hazard.

Keywords: Ground motion simulation, Ambient seismic field, Green's function, Finite source modeling

## Estimation of site amplifications for strong motion stations in Hokuriku district, Japan, based on spectral inversion technique

\*Kazuhiro Somei<sup>1</sup>, Kimiyuki Asano<sup>2</sup>, Tomotaka Iwata<sup>2</sup>, Ken Miyakoshi<sup>1</sup>, Michihiro Ohori<sup>3</sup>

1.Geo-Research Institute, 2.Disaster Prevention Research Institute, Kyoto University, 3.Research Institute of Nuclear Engineering, University of Fukui

To develop the underground velocity structure model for strong motion prediction in Hokuriku district (i.e., Fukui, Ishikawa, and Toyama prefectures), Japan, we evaluate site amplification factors for strong motion stations in this area. Strong motion stations targeted in this study are K-NET, KiK-net, and F-net operated by the National Research Institute for Earth Science and Disaster Prevention (NIED), Japan, and local government Shindo-kei networks in Fukui, Ishikawa, and Toyama prefectures. Owing to dense strong motion stations including local government Shindo-kei networks, we can obtain high density local site amplification factors, especially for the urbanized area, in Hokuriku district.

Site amplifications are estimated by separating source, propagation path, and site characteristics from observed Fourier amplitude spectra based on the spectral inversion technique. We use the vectorial summation of the two horizontal components of Fourier amplitude spectra, which are calculated from the windows of 10.24 s for S-wave records. A moving average of  $\pm 5\%$  window for each frequency point is applied to smooth the amplitude spectra. We choose the F-net SRN station as a reference rock site assuming no site amplification to resolve the trade-off between the source spectra and site effect.

For example of K-NET ISK011, the site amplification from spectral inversion shows the peak between 0.5 and 2.0 Hz with amplification factor from 10 to 20. On the other hand, the 1-D theoretical amplification factor based on the velocity structure model by Japan Seismic Hazard Information Station does not show the peak between 0.5 and 2.0 Hz. However, the 1-D theoretical amplification factor calculated from the improved velocity structure model by using microtremor observations (Asano et al., J. Jpn. Assoc. Earthq. Eng., 15(7), 194-204, 2015) is from 10 to 20 between 0.5 and 2.0 Hz as well as the amplification from spectral inversion. Thus, the obtained high density site amplifications could be useful for performance-checking of existing velocity structure model for each local site, especially for the urbanized area. We identified where we need to improve the velocity structure model by comparing the site amplification obtained from spectral inversion with 1-D theoretical amplification factor from existing velocity structure model in Hokuriku district.

**Acknowledgements:** Strong motion data of K-NET, KiK-net, and F-net provided by NIED are used in this study. We also use the strong motion data from local government Shindo-kei networks operated by Fukui, Ishikawa and Toyama prefectures, Japan. We thank to the staff in these institutes for maintaining and providing the observed records. This study was supported by the Special Project "Integrated Research Project on Seismic and Tsunami Hazards around the Sea of Japan" from the Ministry of Education, Culture, Sports, Science, and Technology of Japan.

**Keywords:** Site amplification, Hokuriku district, Spectral inversion, Strong motion station

## Simulation of characteristic late arrivals after S-wave of local events between Amagasaki and Higashinada in Osaka sedimentary basin

Hiroki Tanaka<sup>1</sup>, \*Tomotaka Iwata<sup>1</sup>, Kimiyuki Asano<sup>1</sup>

1.Disaster Prevention Research Institute, Kyoto University

Tanaka et al.(2014,2015, SSJ fall meeting) analyzed distinctive later arrivals after direct S-waves of local events at Amagasaki strong motion station (CEORKA), and at Ashiya, Fukuike, and Fukae temporary strong motion stations (Iwata et al., 1995). They found that the polarization angles and the linearity of those phases changed systematically with according to the number of reverberations at Amagasaki station, whereas there are not significant phases appeared at other three stations. Those findings suggest that the three-dimensional basin velocity structure affects the reverberation characteristics.

To confirm the observation characteristics, we then conducted the three-dimensional ground motion simulations up to 2Hz using a three-dimensional basin velocity structure model (Sekiguchi et al., 2013) and a double-couple point source model. The simulation reproduces the observation well and proved that those systematic characteristics of the distinctive later phases are caused by the three-dimensional shape of the basin/bedrock interface. From the simulation results, the Amagasaki station locates in the area where the distinctive late phases can be observed clearly. On the contrary, other three stations locates in the area where the S-wave reverberations and the basin-induced surface waves appear simultaneously so as to contaminate clear arrivals.

Keywords: Osaka sedimentary basin velocity structure model, ground motion simulation, multiple-reflection

Strong-motion simulation of the 2015 Southern Oita, Japan, earthquake (Mj5.7) using a 3D structure model including the land and sea-floor topography

Tatsuya Okunaka<sup>2</sup>, Masanao Komatsu<sup>1</sup>, \*Hiroshi Takenaka<sup>1</sup>, Masayuki Yoshimi<sup>3</sup>, Takeshi Nakamura<sup>4</sup>, Taro Okamoto<sup>5</sup>

1.Department of Earth Sciences, Graduate School of Natural Science and Technology, Okayama University, 2.Department of Earth Sciences, Faculty of Science, Okayama University, 3.Geological Survey of Japan, AIST, 4.Japan Agency for Marine-Earth Science and Technology, 5.Department of Earth and Planetary Sciences, School of Science, Tokyo Institute of Technology

Oita prefecture is located in northeastern part of Kyushu Island which is characterized by active subduction of the Philippine Sea plate (PHS) beneath the Eurasian plate and several active volcanoes along with the volcanic front. Oita area has frequently been damaged by large earthquakes and tsunamis since ancient times. From the point of view of disaster prevention, it is important to improve the precision of strong ground motion prediction. In this study we construct a three-dimensional (3D) numerical structure model for simulation of the strong ground motion around Oita prefecture, which includes land and sea-floor topography and a seawater layer as well as subsurface structures of the arc side and the PHS slab, partially based on the J-SHIS model for near-surface structure (National Research Institute for Earth Science and Disaster Prevention) and the Integrated Velocity Structure Model for the arc crust and the slab-top depth model of the PHS (Headquarters for Earthquake Research Promotion, Japan). We then conduct the finite-difference-method (FDM) numerical simulations of strong motion for the 2015 Southern Oita, Japan, earthquake (Mj5.7) whose JMA hypocenter is located in the PHS slab mantle as well as the NIED F-net centroid and which has a strike-slip focal mechanism. We employ the Heterogeneity, Oceanic Layer, and Topography (HOT)-FDM scheme developed by Nakamura et al. (2012, BSSA) to simulate seismic wave propagation in land and ocean areas. From these simulations the best point source is found to be located in the PHS crust, not in the mantle, at depth of about 48 km which is shallower than the JMA hypocentral depth by 10 km. The simulated long-period (2-20 s) motions reproducing observed records demonstrate substantial contributions of thick low-velocity sediment layers in and around Beppu Bay and Oita basin to development of these motions. We also examine the topographic effects on the strong motion by analyzing these simulation results.

Keywords: strong motion, Oita, the 2015 Southern Oita, Japan, earthquake , long-period ground motion, simulation, finite-difference method

## Modeling of the subsurface structure from the seismic bedrock to the ground surface for a broadband strong motion evaluation in Kanto area

\*Shigeki Senna<sup>1</sup>, Atsushi Wakai<sup>1</sup>, Kaoru Jin<sup>1</sup>, Takahiro Maeda<sup>1</sup>, Katsumi Kimura<sup>1</sup>, Hisanori Matsuyama<sup>2</sup>, Hiroyuki Fujiwara<sup>1</sup>

1.National Research Institute for Earth Science and Disaster Prevention, 2.OYO Corp

Sophisticated predictions of strong ground motion are vital when constructing structure models that enable us to evaluate broadband ground motion features. Such models should integrate subsurface structure models for strata shallower than engineering bedrock and deep structure models for strata even deeper. Both such models used to be separately modeled separately so that observation data could be reproduced. In this study, we have created a subsurface structure model applicable from seismic bedrock to ground surface" for whole Kanto area, in attempts to sophisticate subsurface structure models.

We have ever collected bore-hole data and soil physical properties data, and then, by using them, have constructed initial geological models of subsurface structure from seismic bedrocks to ground surfaces in some areas of Japan, which have thicker sedimentary layers.

At present, we are constructing models of subsurface structure in wide area for Kanto and Tokai region of Japan as part of the national project, "Reinforcement of resilient function for disaster prevention and mitigation."

In this study, at first, we collected as many records as possible obtained by microtremor and earthquake observation in the whole Kanto area, including Tokyo. And then, using geological models based on the results of boring surveys as reference, subsurface structure model from seismic bedrock to ground surface was improved based on records of microtremor array and earthquake observation in those areas.

Keywords: strong ground motion evaluation, underground structure models, microtremor observation

## ESTIMATION OF SEISMIC HAZARD FOR STRONG EARTHQUAKES IN TAIWAN

\*YU-WEN CHANG<sup>1</sup>

1.NCREE National Center for Research on Earthquake Engineering of Taiwan

Two main factors that affect the result of ground motion prediction analysis are the existence of the event and site effect. A hybrid procedure, which combines site-dependent ground motion prediction and the limited real time observations, was set up to provide a high-resolution shakemap in a near-real-time manner after damaging earthquakes in Taiwan. The purpose of this paper is to develop the prediction model and procedure considering the characteristic of the damaging earthquake and local site effect, in order to provide an early estimation of potential hazard. In the site-dependent ground motion prediction model, the site effects of each strong motion stations are discussed in terms of a bias function that is site and intensity-level dependent function. Instead of such model, an empirical procedure is supplied to correct the discrepancy of the ground shaking estimated from the attenuation relation and applied to precisely estimate the shakemap of damaging earthquakes for emergency response.

Keywords: shakemap, site effect, ground motion prediction

## Strong motion pulse and building collapse during the 2016 Tainan earthquake

\*Kazuki Koketsu<sup>1</sup>, Hiroaki Kobayashi<sup>1</sup>, Hongjun Si<sup>1</sup>, Loic Viens<sup>1</sup>, Hongqi Diao<sup>1</sup>, Hiroe Miyake<sup>2</sup>

1.Earthquake Research Institute, University of Tokyo, 2.Interfaculty Initiative in Information Studies, University of Tokyo

Ground motions during the 2016 Tainan earthquake have been observed by many stations of P-alert, which is an earthquake early warning system in Taiwan. Looking at the velocity seismograms at stations in Tainan City, a large long-period pulse is found mainly in the EW component to be as large as 100 cm/s at maximum. The Fourier spectrum of the seismogram at the station W21B indicates that the predominant period of this pulse was 1 to 4 s. The collapsed building causing more than 100 fatalities had 16 stories so that its natural period should be 0.8 to 1.3 s according to the relationship of natural period  $T$  and number of story  $N$ :  $T = (0.049 \sim 0.082) \times N$  (Architectural Institute of Japan, 2000). Since the natural period can be longer due to construction defect, this pulse would have had a significant impact on the building. A source inversion of teleseismic body waves revealed that the source fault dipping to the north was located in the east of the city center of Tainan and a rupture consisting of strike-slip and reverse faulting propagated along the strike of the source fault. The westward rupture propagation towards the city center of Tainan went through parts of larger strike slip in the source fault. For a strike-slip fault, it is well known that the rupture directivity effect generates a long-period strong motion pulse in the direction perpendicular to the fault strike. However, the pulse of the Tainan earthquake was dominant in the EW direction, which was parallel to the fault strike. Therefore, a second source fault should be introduced around the area of aftershocks, or the geometry of the original source fault should be revised.

Keywords: Tainan earthquake, strong motion pulse, building collapse

## Simulation of strong ground motions for the 1995 Kobe earthquake based on the pseudo point-source model

\*Atsushi Nozu<sup>1</sup>

### 1. Port and Airport Research Institute

In our country, the characterized source model, which is composed of rectangular subevents generating strong ground motions, have extensively been used for the purpose of predicting strong ground motions (e.g., Kamae and Irikura, 1997). On the other hand, the author (Nozu, 2012) proposed a new source model, namely, the pseudo point-source model. In the model, the spatiotemporal distribution of slip within a subevent is not modeled. Instead, the source spectrum associated with the rupture of a subevent is modeled and it is assumed to follow the omega-square model (Aki, 1967). The source model consists of only six parameters for each subevent, namely, the longitude, latitude, depth, rupture time, seismic moment and corner frequency of the subevent. The model involves much less model parameters than the conventional characterized source model. Once the model parameters are given, by multiplying the source spectrum with the path effect and the site amplification factor, the Fourier amplitude at the site of interest can be obtained. Then, combining it with the Fourier phase of a smaller event, the time history of strong ground motions from the subevent can be calculated. Finally, by summing up contributions from the subevents, strong ground motions from the entire rupture can be obtained.

According to the results of past studies, the model can explain strong ground motions from a mega-thrust earthquake (Nozu, 2012) and an intraslab earthquake (Nagasaka et al., 2014), sometimes better than the conventional characterized source models. Its applicability to short distances, however, could be restricted, because it is expressing the subevent with a point. In addition, the current version of the pseudo point-source model does not consider directivity effects. Therefore, its applicability to shallow crustal earthquakes should carefully be examined by using observed records.

In this study, a pseudo point-source model with three subevents was developed for the Kobe earthquake and strong ground motions were simulated based on the model. According to the results, the pseudo point-source model can explain strong ground motions at KBU and MOT located in Kobe fairly well.

It is well known that strong ground motions in Kobe during the Kobe earthquake were affected by forward directivity (e.g., Kamae and Irikura, 1997). Then the question is why a pseudo point-source model, which does not consider rupture propagation explicitly, can explain strong motions in Kobe. To understand the reason, both Fourier amplitude and phase characteristics of the synthetic ground motions have to be considered. In terms of the Fourier amplitude, rupture propagation theoretically causes a shift in the corner frequency; the corner frequency is increased when the site is affected by forward directivity. In the present pseudo point-source model for the 1995 event, the corner frequencies were determined to be consistent with the observations and, as a result, the selected values of corner frequencies involve any effect of forward directivity. This should be one reason why the model can explain strong ground motions in Kobe. In terms of the Fourier phase, in general, the observed Fourier phase is the sum of the source, path and site effects. In the pseudo point-source model, because the Fourier phase of a small event is used, only the path and site effects are considered. This is equivalent to assuming that the source time function of each subevent is a delta function. Therefore, as long as the Fourier phase is concerned, the pseudo point-source model is actually suitable for the forward sites where the apparent source time function approaches to a delta function. It means that discrepancy is anticipated for the backward

sites. This point should be further studied using records from other crustal earthquakes with better azimuthal coverage.

Acknowledgement: Strong motion data used in this study were observed by the CEORKA.

Keywords: pseudo point-source model, the 1995 Kobe earthquake, strong ground motion

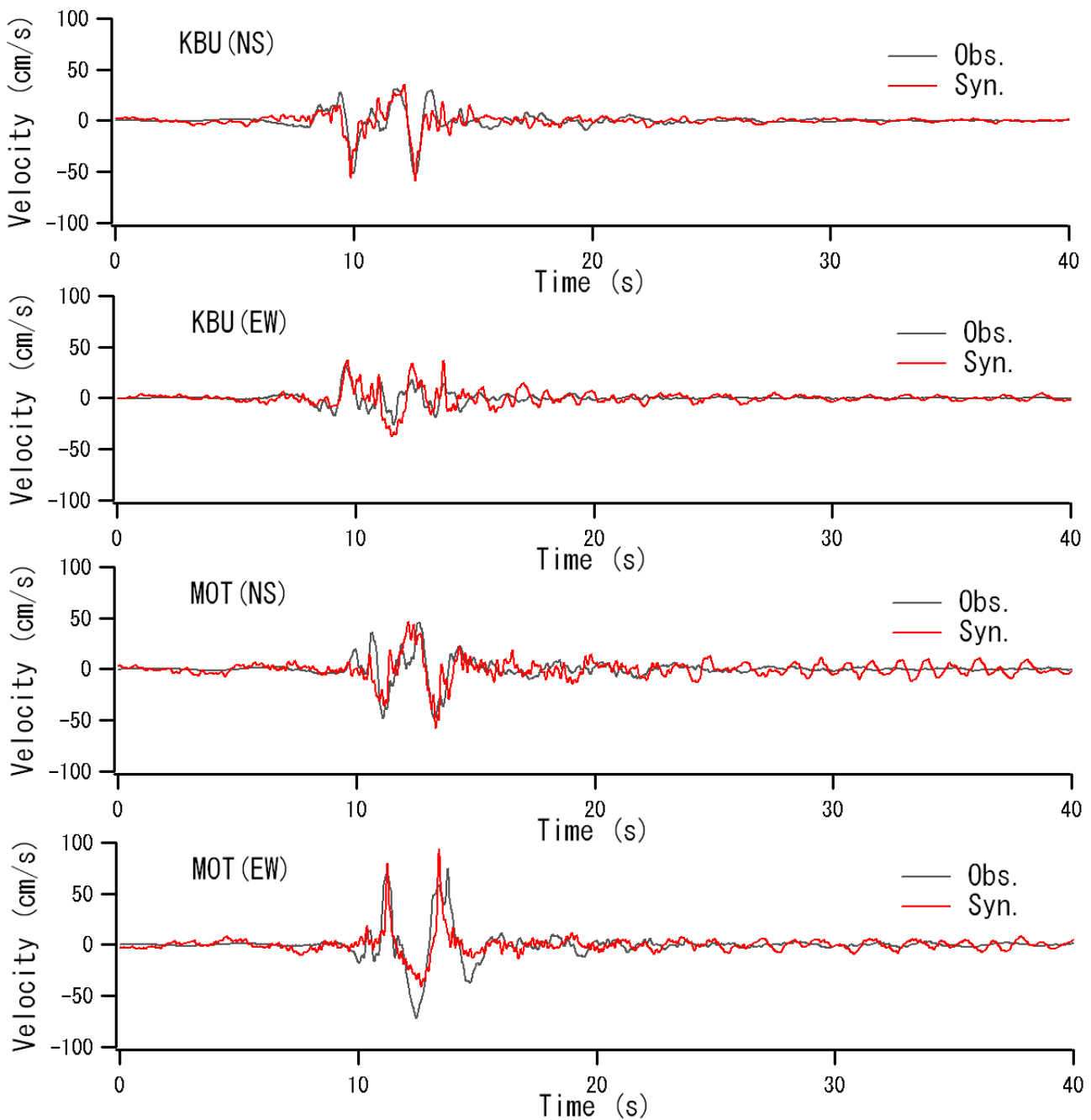


Figure 1 Observed and synthetic velocity waveforms at KBU and MOT

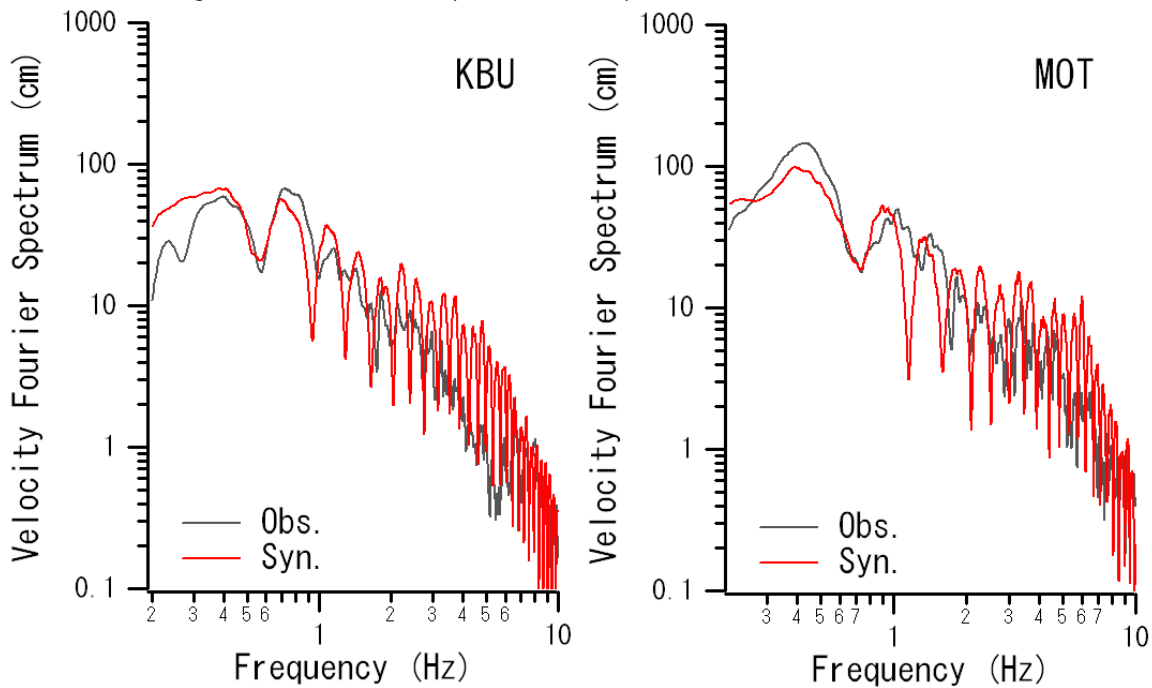


Figure 2 Observed and synthetic Fourier spectra at KBU and MOT



## Characteristics of long-period motion in the Kathmandu Valley during the 2015 Gorkha Nepal earthquake sequence

\*Michiko Shigefuji<sup>1</sup>, Nobuo Takai<sup>1</sup>, Subeg Bijukchhen<sup>1</sup>, Masayoshi Ichiyanagi<sup>1</sup>, Tsutomu Sasatani<sup>1</sup>

1.Hokkaido University

On 25 April 2015, a large  $M_w$  7.8 earthquake occurred along the Himalayan front. The epicenter was near the Gorkha region, 80 km north-west of the Kathmandu Valley, and the rupture propagated eastward from the epicentral region passing through the Kathmandu Valley and reached Sindhupalchok region. The largest aftershock ( $M_w$  7.3) occurred on 12 May 2015 at Sindhupalchok region, 74 km east of the Kathmandu. The Kathmandu Valley is formed by drying of a paleo-lake and consists of thick soft sediment below the center of city. Hence, the Kathmandu city has been damaged not only by near field earthquakes but also far field earthquakes in the past. As for the mainshock, there are 6 strong motion stations (one rock site and five sedimentary sites in the valley (Takai et al. 2016, Bhattarai et al. 2015, USGS 2015)) that recorded the data. Long-period ground motions were recorded on sedimentary sites during the mainshock and aftershocks. We will examine the long-period (2-10 sec) motions in the Kathmandu Valley during the mainshock and aftershocks ( $M_w > 6$ ).

**Mainshock:** The velocity waveforms observed at the rock site KTP show the typical velocity pulse ground motions (5 sec), and there are no clear later phase. The fault parallel component velocity waveform shows a double-sided pulse, while the fault normal and vertical components show a single-sided velocity pulse. The Kathmandu Valley is located at a very close distance (~10 km) to the rupture area and the estimated large slip areas exist near the valley (Galetzka et al. 2015). Therefore, the observed velocity pulses may be effected by this fault rapture process. The vertical component ground velocities at the sedimentary sites are nearly the same as that observed at the rock site KTP. On the contrary, the horizontal ground velocities at the sedimentary sites have a long duration with conspicuous long-period oscillations. We tried 1-D amplification simulation for sedimentary sites using with KTP record as input motion to examine the cause of this long period motion (Bijukchhen et al. 2016) and we could know the importance of examining the effect of 2,3-D valley basement structure.

**Largest Aftershock:** We could recognize peaks around 0.1 Hz in the Fourier velocity spectra for all stations. Therefor we applied low-pass filter (0.2 Hz) for the velocity waveforms and plotted particle motion. Including rock site KTP, we observed retrograde motion just after initial S-wave motion from these particle motion. These motions should have been controlled by propagation of Rayleigh wave; the Rayleigh waves were also observed in the other shallow aftershocks ( $\Delta$ ~80 km). We examined this phenomenon by the Discrete Wave Number method (Takeo, 1985) with 1-D velocity structure (Monsalve et al. 2006) and GCMT source mechanism. The simulated waveforms have good fitness with observed records and we could grasp the excitation of Rayleigh waves.

In this examination, we recognize the difference in excitation and propagation of long-period ground motions during the mains hock and aftershocks. We will study the excitation and propagation of surface wave in the Kathmandu basin in detail.

**Keywords:** The 2015 Gorkha Nepal earthquake sequence, Kathmandu Valley, Strong motion records, Long-period motion

## Simulation of long-period ground motions in the Kathmandu basin during the 2015 Gorkha, Nepal, earthquake

\*Hisahiko Kubo<sup>1</sup>, Yadab Prasad Dhakal<sup>1</sup>, Wataru Suzuki<sup>1</sup>, Takashi Kunugi<sup>1</sup>, Shin Aoi<sup>1</sup>, Hiroyuki Fujiwara<sup>1</sup>

1.National Research Institute for Earth Science and Disaster Prevention

The 2015 Gorkha earthquake ( $M_w$  7.9) occurred in the central Nepal at 06:56 on 25 April 2015 (UTC), and caused extensive damage to the Nepal society. During the 2015 Gorkha earthquake, strong ground motions with predominant components at 4–5 s period were observed in the Kathmandu basin (e.g. Galetzka et al. 2015; Takai et al. 2016). The waveform observations inside and outside the Kathmandu basin indicated that the characteristic long-period ground motions were caused by both effects of the source and Kathmandu basin. In order to investigate how well the long-period ground motions can be reproduced by available source and structure models, we carried out the waveform simulation in long period ( $> 4$  s) at KATNP site located in the Kathmandu basin using the source model obtained by the joint source inversion and the estimated 1D velocity structure model for the Kathmandu basin.

The source process of the 2015 Gorkha earthquake was estimated by the fully Bayesian multiple-time-window source inversion (Kubo et al. 2016) with jointly using near-field waveforms, teleseismic waveforms, and geodetic data. The estimated seismic moment and maximum slip are  $7.5 \times 10^{20}$  Nm ( $M_w$  7.9) and 7.3 m, respectively. The total source duration is approximately 50 s. The derived source model has a unilateral rupture towards east and a large slip area north of Kathmandu with the maximum slip.

The 1D deep subsurface velocity structure beneath KATNP was constructed by a trial-and-error process to reproduce the peak period on the long-period side of the horizontal-to-vertical spectral ratios of coda waves from eight aftershock recordings. The available geological and geophysical information were also utilized in this process. In this basin structure model, the thickness of low-velocity ( $V_s < 500$  m/s) layers is approximately 460 m.

Using the derived source model of the 2015 Gorkha earthquake and the structure model of the Kathmandu basin, we carried out the simulation of the long-period ground motions during the 2015 Gorkha earthquake. The simulation demonstrated that the major features of the observed waveforms can be reproduced by our source and basin structure models.

[Acknowledgments] The high-rate GPS data provided by the Department of Mines and Geology, Tribhuvan University, and California Institute of Technology, and the strong motion data observed by the USGS were used in this study.

Keywords: Long-period ground motions, The 2015 Gorkha earthquake, The Kathmandu basin, Waveform simulation

Detection of nonlinear site response using the main shock and its aftershocks of the 2015 Gorkha, Nepal Earthquake recorded at the DMG site of the Kathmandu Valley, Nepal

\*Mukunda Bhattarai<sup>1</sup>, Lok Bijaya Adhikari<sup>1</sup>, Umesh Prasad Gautam<sup>1</sup>, Bharat Prasad Koirala<sup>1</sup>, Chintan Timsina<sup>1</sup>, Toshiaki Yokoi<sup>2</sup>, Takumi Hayashida<sup>2</sup>, Laurent Bollinger<sup>3</sup>

1.Department of Mines and Geology, Ministry of Industry, Nepal , 2.International Institute of Seismology and Earthquake Engineering, Building Research Institute,Japan, 3.Departement Analyse Surveillance de l'Environnement, Commissariat Energie Atomique, France

We have tested the occurrence of non-linear behavior of soil at the DMG site using the accelerograms of the main shock and its aftershocks during the 2015 Gorkha, Nepal Earthquake. The DMG accelerometric station is installed on the surface at the concrete slab of the single-storey office building in the central part of the Kathmandu Valley filled by sediments. We calculated the horizontal to vertical spectral ratios of S-waves part of the earthquake records (S-H/V) which is expected to provide information about the ground response. Then we calculate the degree of non-linearity (NDL) (Noguchi and Sasatani 2008) for the main shock and its 5 aftershocks in the frequency range from 1 Hz to 10 Hz. It is found that DNL of the main shock record clearly different from those of the aftershocks records. The PGA-DNL plot shows that the main shock runs off from the trend formed by the aftershock records.

Based on the above study we guess that non-linear behavior took place during the main shock of the 2015 Gorkha, Nepal Earthquake.

Keywords: Non-linear site effect, Degree of non-linearity, Gorkha earthquake, Kathmandu Valley

Relationship between Irregularity of Boundary of Subsurface Geology and Spatial Variation in Peak Periods of Horizontal to Vertical Spectral Ratio of Microtremors  
-A Study Based on Numerical Simulations-

\*Kentarō Motoki<sup>1</sup>, Tetsushi Watanabe<sup>1</sup>, Kenichi Kato<sup>1</sup>

1. Kobori Research Complex

Earthquake motions on an irregularly layered subsurface geology (hereafter irregular site) sometimes show a higher amplification than on a stratified media (hereafter flat site) due to, for example, a focusing effect of seismic waves. An exploration of depth distribution of geological boundary is necessary for a reliable estimation of amplification factor at an irregular site, but it is too costly to make such a survey at every site in practice. Before a detail survey, a simple method to sort out irregular site from flat site is desired for insufficient geological information sites. Focusing on spatial variation in peak periods of horizontal to vertical spectral ratios (hereafter HVSRs) of microtremors, we showed in Motoki et al.(2012) that the values of coefficients of variation (hereafter CVs) were obviously separated between irregular sites and flat sites. In this report, we performed 2 investigations using numerical simulations with respect to a relationship between CVs and irregularity of subsurface geology.

First, in order to reveal what kind of parameters of subsurface geological model affected amplitude of CVs, we analyzed a sensitivity for CVs by numerical simulation with various parameters. The basic geological model was constructed based on results of drilling method at Nabari site where mobile microtremor measurements were also conducted. CVs of simulated motions with the basic model are almost consistent with the CVs by the observations. We found out that slope angles and horizontal sizes of irregularity affected amplitudes and inflection distances of CVs.

Second, we directly compare CVs to irregularity of subsurface geology, using results of simulated microtremors and geological models. For a comparison, we converted CVs to a power spectral density (hereafter PSD) via a semivariogram, which were frequently used in geostatistics. The PSD estimated from the CVs showed a good agreement with the PSD calculated from geological model in the wave number range corresponding to interstation distances to estimate the CVs. Note that we can say CVs reflect irregularity of subsurface geology.

We evaluated the difference of CVs by fluctuating irregularity of subsurface geology through numerical simulations. Consequently, we found that CVs can be an index of the irregularity, and we will suggest a procedure and a threshold in future works.

Keywords: Microtremors, Peak period of H/V, Spatial variation, Coefficients of variation, Power spectral density

Estimation of S-wave velocity structures of an irregular ground using H/V spectral ratio  
~Case study in the middle coast of Miyazaki prefecture~

\*Kyosuke Okamoto<sup>1</sup>, Seiji Tsuno<sup>1</sup>, Masahiro Korenaga<sup>1</sup>

1. Railway Technical Research Institute

S-wave velocity structures have been estimated from dispersion curves of phase velocity, H/V spectral ratios, etc., using microtremor exploration technique. However the estimations are originally based on the assumption that underground structures have stratified horizontally. So, if structures have irregular, e.g., layers incline or discontinue, the structures estimated under the assumption of horizontal stratification have errors to some extent due to perturbation of wave filed at the irregular. On the other hand, it has been known that seismic waves are likely to be amplified at the irregular structures since the various seismic waves interfere with each other. So, accurate estimation of the irregular structures is needed for disaster prevention. Seismic reflection and boring surveys are powerful tools to estimate the irregular structures since boundaries of the structure are directly imaged. However sometimes they have difficulties in cost and space for their application, especially surveys of a wide range of areas are limited. Here, we focus on H/V spectral ratios, which are relatively easy to measure a wide range of areas with a small budget, to estimate a dipping structure.

In this study, we applied microtremor explorations and observed earthquake ground motions (from Sep. to Nov., 2015) along Miyazaki maglev test line (Railway Technical Research Institute), where an irregular structure has been estimated by a preceding study, to examine the applicability of microtremor explorations to irregular structures. The microtremor explorations and the observations of earthquake ground motions were conducted at 8 points with about 290m intervals along a 2km survey line, whose center is the irregular point. We estimated S-wave velocity structures at each observation points by the SPAC method, and confirmed that the dipping structure exists at the location pointed out by the preceding study. We validated the structures estimated at each observation points by checking the similarity of the converted seismic waves on the basement. We also confirmed that the theoretical H/V spectral ratios of the observation points calculated by the multiple reflection theory agree with the observed H/V spectral ratios well. It suggests that H/V spectral ratios can illuminate the dipping structure. However, the theoretical and observed H/V spectral ratios disagree with largely each other around the edges of the dipping structure. One of the causes of this disagreement is that a complex wave filed is produced by reflecting waves, higher modes of surface waves, etc., at the dipping structure, and it cannot be accounted by the assumption of horizontal stratification.

To examine the original locations of the disturbance in the wave field, we synthesized the wave field using a numerical simulation using the estimated structure model. We divided the synthesized wave at the edges of the dipping structure into surface wave and the others (reflections, refractions and etc.), then, we calculated the original locations of the latter waves based on the method of back propagation. As a result, it was revealed that part of the dipping structure within one-wavelength from the issued receiver (here, the receiver at the edges) gives major effect in terms of the disturbance. We also confirmed that the H/V spectral ratio calculated using the divided surface wave agrees to the theoretical H/V spectral ratio, which is based on the assumption of horizontal stratification. It implies that the disturbance in wave fields (reflections, refractions, etc.) perturb the observed H/V spectral ratios.

In this study, we interpreted using a 2-D model. As a further discussion, it is necessary to consider 3-D effects.

Keywords: microtremor exploration, Earthquake ground motion, dipping structure

## A Method of Estimating Incident Wave Considering Nonlinear Response of the Non-uniform Surface Ground

\*Shotaro Yamada<sup>1</sup>, Toshihiro Noda<sup>2</sup>, Akira Asaoka<sup>3</sup>, Yoshihiro Sawada<sup>3</sup>

1.Civil Engineering, Nagoya University, 2.Disaster Mitigation Research Center, Nagoya University,  
3.Association for the Development of Earthquake Prediction

When a strong earthquake motion is the case, whether a seismometer is installed underground or on a ground surface, any information recorded through the seismometer should naturally reflect the influence of highly nonlinear mechanical behavior of a surface ground that usually exhibits non-uniform multi-layered system. In other words, every strong ground motion analysis cannot be performed without the use of soil mechanics that describes nonlinear mechanical behavior of a non-uniform surface ground system.

In recent years, the elasto-plastic finite deformation computation of a soil water coupled system<sup>1)</sup> is utilized for the analysis of surface ground behavior from deformation to failure including soil liquefaction that occurs during/after a strong 'quake. In this research, a method of estimating input earthquake motion at an engineering base surface is newly presented from the records of seismometer at the basement that should reflect nonlinear mechanical behavior of a non-uniform multi-layered surface ground.

In the presented method, the existence of a semi-infinite purely elastic ground is assumed below the so-called "horizontal engineering base surface" along which viscous boundary<sup>2), 3)</sup> is introduced at the bottom of a surface ground system. The earthquake motion is input at the bottom of surface ground through the viscous boundary. Let  $E$  be the upward transmitting wave, while  $F$ , the downward wave. In the usual "viscous boundary analysis", the  $E$  is assumed at the viscous boundary as an input data and the whole surface ground motion is solved. As the results, the  $E+F$  is obtained at viscous boundary. Therefore, in usual computation, by giving  $E$ , at a viscous boundary,  $E+F$  is calculated at any point on the boundary. This  $E+F$  will be recorded if a seismometer is installed at the engineering base surface. However, the input data  $E$  is always to be assumed. The recorded and then observed  $E+F$  cannot be the  $2E$ , because  $F$  includes every influence of both nonlinear mechanical behavior of ground motion and non-uniform geometrical shape of a multi-layered surface ground system. In this research, a method is newly proposed of calculating  $E$  by the use of observed  $E+F$  as an input data.

It is naturally considered that incident wave  $E$  should be uniformly distributed on an engineering base surface. This constrained motion at the bottom of surface ground is introduced through a "method of Lagrange multiplier", in which Lagrange multiplier is to give the constrained force. Therefore,  $E$  is solved, from time to time, by calculating Lagrange multipliers.

For the verification of the method, the need of measurement of  $E+F$  at many locations on/in the surface ground is particularly emphasized in this research.

### References

- 1) Noda, T., Asaoka, A. and Nakano, M. (2008): Soil-water coupled finite deformation analysis based on a rate-type equation of motion incorporating the SYS Cam-slay model, *Soils and Foundations*, 45(6), 771-790.
- 2) Lysmer, J. and R., L., Kuhlemeyer (1969): Finite dynamic model for infinite media, *ASCE, EM4*, 859-877.
- 3) Noda, T., Takeuchi, H., Nakai, K. and Asaoka, A.(2009):Co-seismic and post-seismic behavior of an alternately layered sand-clay ground and embankment system accompanied by soil disturbance, *Soils and Foundations*, 49(5), 739-756.

Keywords: incident wave, observed wave, engineering base surface, surface ground, nonlinear analysis, viscous boundary

## Numerical realization of surface waves and assessing their influence on liquefaction using 2D effective stress analysis

\*Kentaro Nakai<sup>1</sup>, Toshihiro Noda<sup>2</sup>, Akira Asaoka<sup>3</sup>, Sho Ozaki<sup>1</sup>

1.Graduate School of Engineering, Nagoya University, 2.Disaster Mitigation Research Center, Nagoya University, 3.Association for the development of earthquake prediction

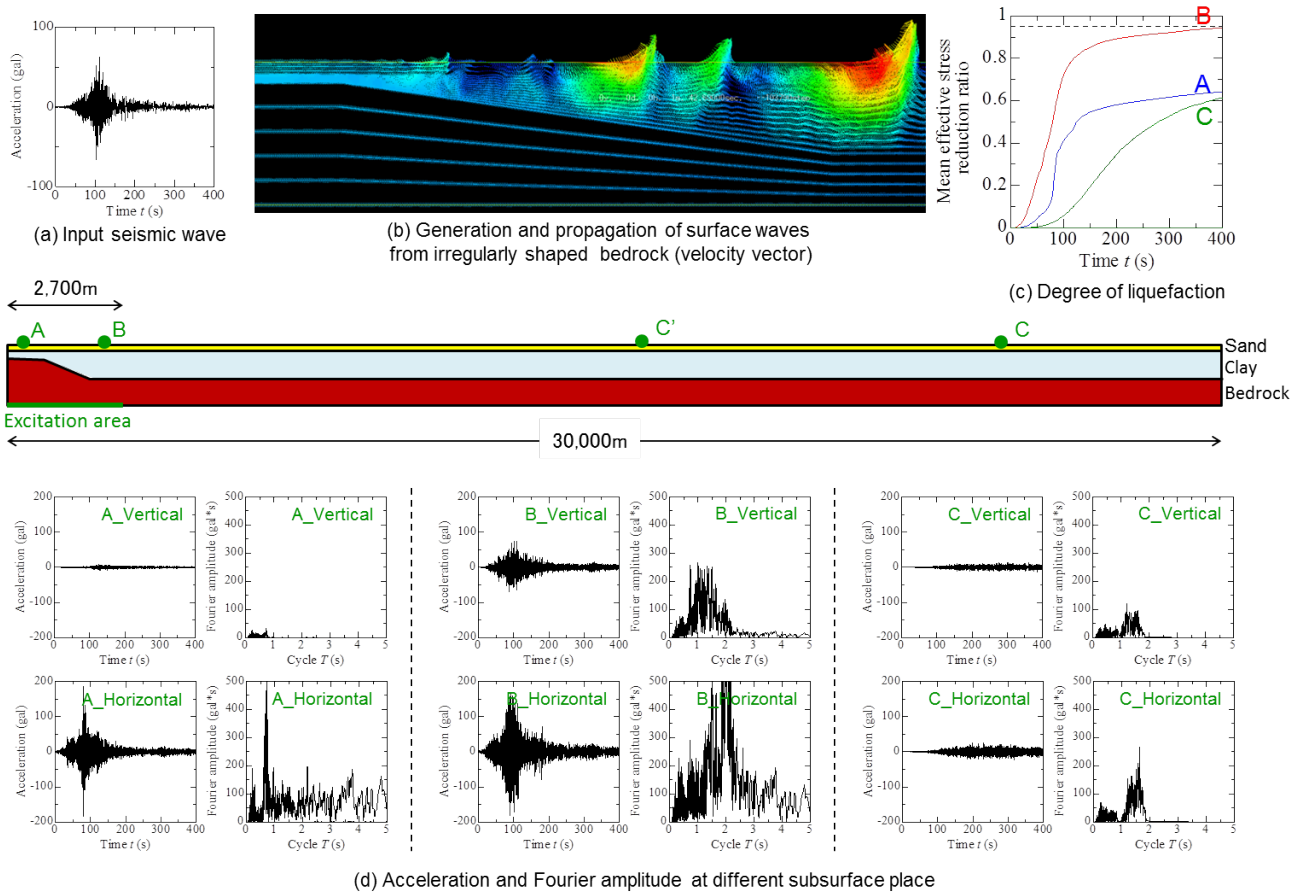
One of the important characteristic of surface waves is that distance attenuation is small compared with P-wave and S-wave. Therefore, it can propagate to hundreds of kilometers away from epicenter, and leads to a post-motion phenomenon of relatively large continued tremors even after the primary motion has ended. Moreover, complex interference between the surface waves and the body wave causes extensive and localized seismic damage. However, the influence of surface waves on liquefaction damage is not fully understood yet. This report tries to reproduce surface waves and assess its influence on liquefaction with the use of 2D elasto-plastic seismic response analysis considering the effect of irregularly shaped bedrock. The analysis code employed in this report was the soil-water coupled finite deformation analysis code GEOASIA<sup>2)</sup>, which incorporates an elasto-plastic constitutive model<sup>1)</sup> that allows description of the behavior of soils ranging from sand through intermediate soils to clay under the same theoretical framework.

The ground model was prepared with its height 100m and width 30,000m. Bedrock was assumed to be inclined at extreme left side of the ground. Stratum organization was assumed to be Pleistocene layer in deep part, above which was a sensitive soft clayey layer, followed by a loose sandy layer with reference to Urayasu ground<sup>3)</sup>. The hydraulic boundary was set that the ground surface coincided with water level was set up as water pressure equal zero. The bottom face and the two lateral faces were assumed to be undrained boundaries. The seismic wave that was observed at a depth of about G.L. -36 m at Shinagawa observation point of the Tokyo Bureau of Port and Harbor (see Fig.1 (a)) was input as a 2E-wave in the horizontal direction only at the bottom face beneath the inclined bedrock area. In addition to establishing simple shear deformation boundaries at the two lateral ends of the boundaries, a viscous boundary equivalent to  $V_s=400$  m/s was set up at the bottom face of both excitation and non-excitation area. Fig.1 (b) illustrates the velocity vector distribution 100 sec after the earthquake occurrence. Surface waves are generated at the base end section of the inclination which shows orbit in a counterclockwise direction with ongoing wave propagation to the right-hand side. Fig.1 (d) illustrates the acceleration responses at locations A, B and C. Location A sited left side of inclined bedrock shows smaller acceleration compared with location B and doesn't generate vertical motion. On the other hand for location B, in addition to the generation of vertical motion, duration and maximum acceleration are enlarged for horizontal motion caused by the propagation of surface waves. Moreover, location C sited 20,000km away from excitation area still observed acceleration response, although the maximum amplitude is around 30gal. This seismic motion can be regarded as surface waves so that the similar acceleration response can be observed at location C'. Fourier amplitude of the surface waves is dominant at slightly long-period around 1.7 sec. Fig.1 (c) illustrates mean effective stress reduction ratio at each location. Although the reduction ratio at location A didn't increase so much, location B gradually increases even after the primary motion and finally reaches to 95% which indicates liquefaction. Gradual increase was caused by the complex interference between the surface waves and the body wave. Moreover, location C is also gradually increased to the extent of 60% even the observed seismic motion is not so large. This result indicates that the location C has a risk of delayed-liquefaction damage with additional aftershock excitations.

1) Asaoka, A. et al. (2002): An elasto-plastic description..., S&F, 42(5), 47-57.

- 2) Noda, T. et al. (2008): Soil-water coupled ..., S&F, 48(6), 771-790.
- 3) Nakai, K. et al. (2014): Liquefaction damage expansion..., JGUM, SSS23-19.

Keywords: surface wave, liquefaction, irregularly shaped bedrock, effective stress analysis



## Earthquake Fatalities Mapping for the Eastern Asia Earthquake and Volcanic Hazards Information Map

\*Masayuki Yoshimi<sup>1</sup>, Yuzo Ishikawa<sup>1</sup>, Shinji Takarada<sup>1</sup>, Jeol Bandibas<sup>1</sup>, Tadashi Maruyama<sup>1</sup>, DAN MATSUMOTO<sup>1</sup>, Takashi AZUMA<sup>1</sup>, Ryuta FURUKAWA<sup>1</sup>, Akira Takada<sup>1</sup>, Yasuto Kuwahara<sup>1</sup>, Eikichi Tsukuda<sup>1</sup>

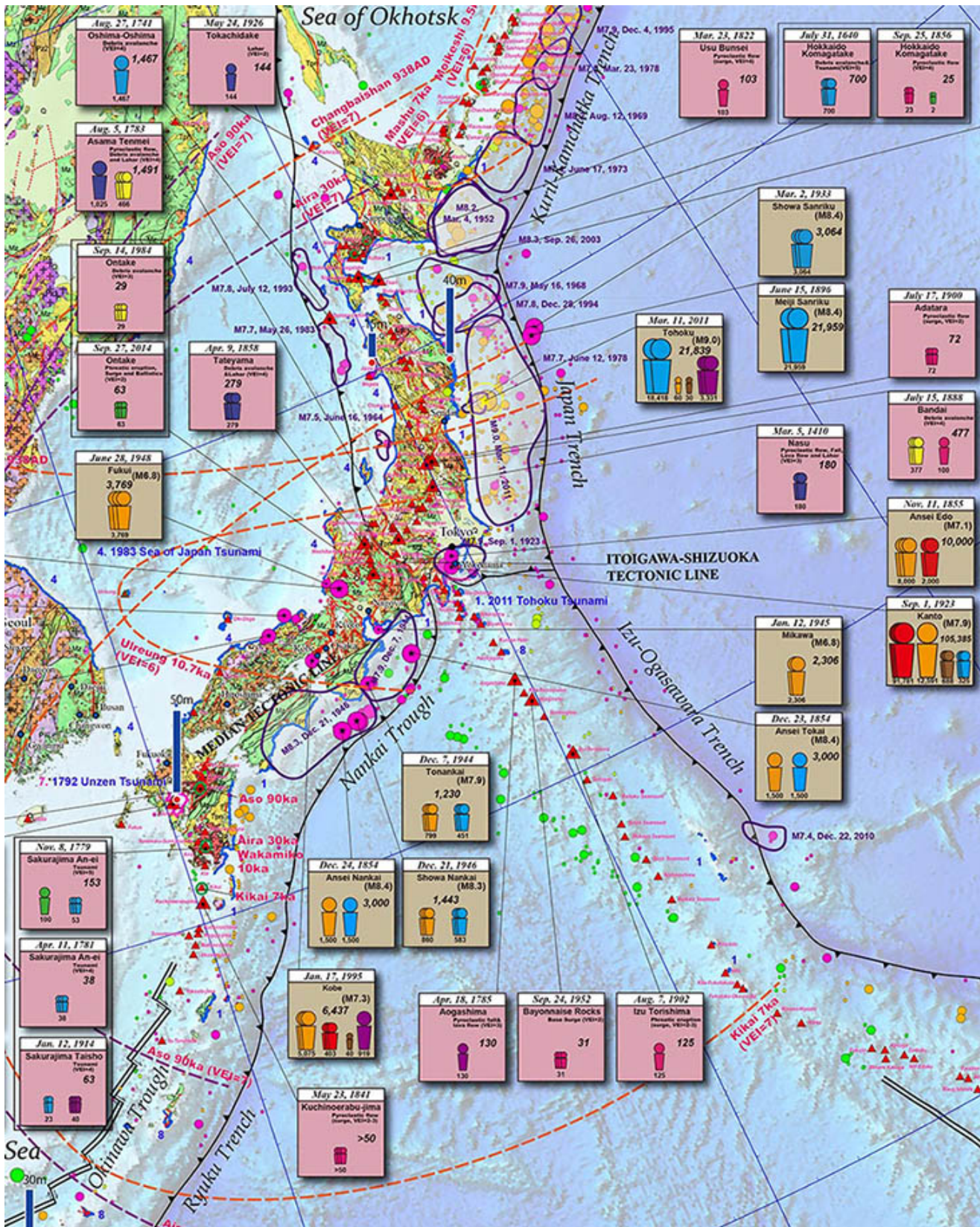
1.Geological Survey of Japan, AIST

The Eastern Asia Earthquake and Volcanic Hazards Information Map is published in May 2016. This map illustrates geology and tectonics, active faults, earthquakes hypocenters and source areas, fatalities of major earthquakes, tsunami hazards, distribution of volcanoes, calderas, pyroclastic falls and ignimbrites, and fatalities of major volcanic events. We believe that this hazards information map will provide useful information for earthquake, tsunami, and volcanic disaster mitigation efforts.

Earthquake fatalities map is one of the major contents, which has been compiled to facilitate visual understanding of earthquake disasters in terms of their number of fatalities (deaths) and the main causes of deaths. Major disastrous earthquakes in terms of number of fatalities are selected in each country or region: all the recent (after 1850) events with fatalities more than 1,000 (hereafter, F1000 event) are included; for a country with less than three F1000 events, two F100-F10 events are added; for a country with no F1000 events, up to two F100 events or one worst earthquake with fatalities are added. The number of fatalities is categorized by five causes; structure (building) damage, tsunami, landslide, fire, and others (related death), when possible. It is important to understand that an earthquake and ground motions do not directly kill people, but vulnerable structures, fire, landslide, or tsunami do. The number of fatalities is mainly based on the Significant Earthquake Database (NGDC/WDS) provided by NOAA, and individual reports of each earthquake, if any.

The contents of the Information Map are planning to be implemented on the online hazard information system (<http://ccop-geoinfo.org/G-EVER>). We are going to collect more data or reports to make the map more reliable.

Keywords: Eastern Asia, disastrous earthquake, number of fatalities



## Age-dependent Mortality in the 2011 East Japan Earthquake -Further Revision of Traditional Mortality at Attack by Tsunami

\*Yutaka Ohta<sup>1</sup>, Maki Koyama<sup>2</sup>, Tomoko Shigaki<sup>3</sup>

1.Tono Research Institute of Earthquake Science, 2.River Basin Research Center Gifu University,  
3.Institute of Elderly Housing Science

### 1. Preface

This paper reports a further development of known age-band specific mortality equation at attack by a tsunami. The equation in a certain age-bound has been written as

Mortality (%) = Number of deaths / Number of people concerned (1).

The equation looks therefore apparently simple enough. But, the reality is different from what we see in the equation, since the equation itself gives no special constraint. Incidentally, there come two essential issues to keep in mind at application.

The first one gives very low mortality for infants and children in case when a straight application of the equation is made to the 2011 giant tsunami, and on the contrary it gives very high mortality for aged people, which seems far illogical.

The second issue requiring careful treatment is how to fix the appropriate population concerned. Employing either prefectural or municipal census data with age-specific population by 5-year intervals is very convenient because of its easy accessibility, but we should be careful on whether or not those data are responsible for the real number of population attacked by a tsunami. As has already been criticized by Sawai<sup>1)</sup>, we should keep in mind of regulation of population to be suited to have direct comparisons in one event or in plural numbers of natural disasters as of earthquakes, tsunamis and, etc.

### 2. Methodology to overcome the above-stated two serious issues

In order to overcome the first issue we applied the Ozaki's method<sup>2)</sup> with a little modification. The essential point in his method is to give a special weight to a comparison of the mortality attacked by the natural disaster as tsunami, with that in one ordinary year during which no devastating disaster attacks. Thus we can get rid of any misunderstandings<sup>3)</sup>.

To overcome the second issue we finally adopted the outstanding outcomes by Koyama and her colleagues<sup>4)</sup> who succeeded counting of residents in the area inundated by the tsunami and in the area where their living houses were swept away. Since we have known by Hatori's work<sup>5)</sup> that the residents killed are mostly living in the swept-away houses, we placed higher priority on the number of residents living in the swept-away area.

### 3. Concluding Remarks

The finally obtained are summarized as in the followings.

- 1) For the mortality evaluation by the attack of tsunami, it is necessary to have a comparative study with the mortality in one ordinary year with no disasters.
- 2) Reasonable population at the mortality evaluation by tsunami is to count the number of occupants living in the swept-away houses by the tsunami.
- 3) We can evaluate the severity of mortality by tsunami just by ratio with one ordinary year with no significant disasters, and we are easy to understand that infants' mortality at attack by tsunami is far severer than that in one ordinary year.
- 4) In spite of the fact as in 3), in a few areas nearby Kamaishi city in Iwate Pref., we found the mortalities are relatively smaller, which suggests the effectiveness of special training frequently guided by Katada<sup>6)</sup>.
- 5) We have recognized a certain positive correlation between the derived

mortalities and tsunami heights.

#### References

- 1) Ozaki, kousei no shihyou, 59, 2012 (in Japanese).
- 2) Ohta, Koyama and Shigaki, Mortality in the 2011 East Japan Earthquake (2~6). JpGU Meeting, 2013-15.
- 3) Sawai, M., Who is vulnerable during tsunamis? , 1-18, 2012, ESCAP Spec. Rep.
- 4) Koyama et al, Municipality's mortality rate according to Inundation level and age on the 2011 Tohoku earthquake, Earthq. Engr., Japan Civil Engr., 2012.
- 5) Hatori, Damage rate of Residential Houses by a Tsunami, BERI, 59, 1984.
- 6) Katada; Hito ga shinanai bousai 2012, Shueisya.

Keywords: East Japan Earthquake, Tsunami, Mortality, Critical Revision

## Estimation of source model of the 1931 NISHI-SAITAMA earthquake using long-period ground motion at Hongo in Kanto basin

\*Ryosuke Chujo<sup>1</sup>, Hiroaki Yamanaka<sup>1</sup>, Kosuke Chimoto<sup>1</sup>, Kazuyoshi Kudo<sup>2</sup>, Kazuki Koketsu<sup>3</sup>, Hiroe Miyake<sup>3</sup>

1.Interdisciplinary Graduate School of Science and Engineering, Tokyo Institute of Technology,  
2.College of Industrial Technology, Nihon University, 3.Earthquake Research Institute, University  
of Tokyo

The 1931 Nishi-Saitama earthquake occurred in the northwestern part of Saitama prefecture on September 21, 1931 with a magnitude of 6.9. This is one of the most destructive shallow crustal earthquakes in the Kanto district in the last 100 years. Heavy building damage was experienced in the epicentral area during the quake. It is important from the viewpoint of disaster mitigation to know the source model of the earthquake for considering ground shaking during future events. Abe (1974) estimated the focal depth according to observed P-wave travel time in distant station and suggested shallow focal depth. However, the focal depth has not been precisely understood. In this study, we tried to estimate a source model of the 1931 Nishi-Saitama earthquake by comparing a long-period seismogram observed in Hongo, Tokyo, which is the only seismogram recorded completely in the Tokyo Metropolitan area with synthetic seismograms simulated by a 3D finite differential method considering recent detailed model of the Kanto basin. It is clarified that the main part of the observed long-period seismogram is composed of surface waves affected by the three-dimensional effect of the sedimentary layers in the Kanto basin. We also found good agreement between the calculated and observed seismograms, when the depth of the source fault is set to be in a range of 20-30 km with a rupture propagating from the bottom edge of the center of the fault.

Keywords: The 1931 Nishi-Saitama earthquake, long-period seismogram, focal depth

## Source inversion using EGF for the 2008 Iwate-Miyagi earthquake based on precisely relocated aftershock distribution

\*Yoshiaki Shiba<sup>1</sup>

1. Central Research Institute of Electric Power Industry

During the 2008 Iwate-Miyagi Nairiku earthquake, the peak ground accelerations at several stations exceeded 1G. The faulting mechanism of this event was considered to be the west-dipping reverse fault from the CMT solution, initially estimated aftershock distribution and the location of surface deformation. On the other hand another source model that the conjugate faults are ruptured simultaneously has been proposed recently based on the precisely relocated aftershock distribution (Yoshida, 2013) and the geodetic data detected by the GPS and the In-SAR (Abe et al., 2013). The source modeling using strong motion data was also carried out assuming conjugate fault plane, and significant slips are estimated on both the fault planes (Hikima and Koketsu, 2013). In this study the conjugate fault planes model and west-dipping plane model are prepared based on the aftershock locations by Yoshida (2013) and the waveform inversion using the empirical Green's function is applied.

The initial conjugate fault model for the inversion analysis in this study consists of three planes. For the west-dipping fault I assume two planes with different strike and dip angles according to the latest aftershock distribution and the trace of surface deformation. Furthermore the east-dipping conjugate fault plane is added. Observed records from two aftershocks of Mj 4.2 and 4.0 occurring near the northern and southern fault planes are adopted for the empirical Green's functions. Velocity motions of two horizontal components for 20 near-source stations are used for the source inversion in the frequency range from 0.1 to 1 Hz. The difference of the radiation patterns between the main shock and EGFs are corrected following Boore and Boatwright (1984). The obtained source model from the conjugate fault indicates large slips mainly in the southern part from the hypocenter on the west-dipping northern fault plane and secondary large slips on the east-dipping fault. The slip distribution of the source projected on the horizontal plane shows that the slips on the conjugate faults are complementary. The maximum slip reaches 5.3 m. While the source model with west-dipping fault plane implies the main slips are estimated on the almost same area and the peak value is 6.1 m. For both cases though the asperity on the west-dipping fault is located beneath the trace of observed surface deformations, it lies in rather deeper position. It is considered to be consistent with the fact that the surface fault ruptures are not observed clearly.

Keywords: The 2008 Iwate-Miyagi earthquake, source inversion, empirical Green's function

## Dynamic source parameters of the 2008 Iwate-Miyagi inland earthquake inferred from kinematic source model

\*Kunikazu Yoshida<sup>1</sup>, Ken Miyakoshi<sup>1</sup>, Kazuhiro Somei<sup>1</sup>

### 1. Geo-Research Institute

The spatial and temporal distributions of the stress on the fault planes of the 2008 Iwate-Miyagi Inland earthquake ( $M_0=2.4 \times 10^{19}$  Nm,  $M_w$  6.9) is calculated from kinematic inversion result using a three-dimensional finite difference method for solving the elastodynamic equations. This event is dip-slip with surface rupture. We analyze the relations between stress and slip for all grid positions on the fault, and use these relations to infer the friction law for the rupture dynamics. Then, the dynamic source parameters were also determined. The distributions of the dynamic parameters on the fault are very heterogeneous. Average of dynamic stress drop on the asperity is ~13 MPa. Average fracture energy over the entire fault is estimated ~6 MJ/m<sup>2</sup>, which coincides with the seismic moment relationship by Tinti et al. (2005). The fracture energy is proportional to the final slip. In general, the stress drop and fracture energy are correlated with the slip distribution. Rupture time on each subfault is determined based on peak stress time. The rupture propagation was gradually accelerated in the asperity, and was delayed along the surface. For the surface rupture earthquake, we estimate small or negative stress drop and small fracture energy, where large slip is estimated along the surface.

Acknowledgements: This study was based on the 2015 research project 'Improvement for uncertainty of strong ground motion prediction' by the Nuclear Regulation Authority (NRA), Japan.

Keywords: The 2008 Iwate-Miyagi inland earthquake, Dynamic source parameter, Kinematic source model

## Dynamic source parameters of the 2013 Tohigi-ken hokubu earthquake inferred from kinematic source model

\*Kazuhiro Somei<sup>1</sup>, Ken Miyakoshi<sup>1</sup>, Kunikazu Yoshida<sup>1</sup>

### 1. Geo-Research Institute

Revealing detailed source rupture processes for past large earthquakes is an essential study to make the advanced characterized source model for reliable strong motion prediction. Though the concept of characterized source model in a "recipe" is based on the result from kinematic source model, the physics of source rupture process in nature is represented by dynamic model, which is described as an evolution of shear stress with the frictional property on the fault. For understanding a more physically accurate model to make the ground motion, the study on strong motion simulation with dynamic source model has been developed in decades. In this study, we estimate the spatio-temporal stress change and dynamic source parameters on and off the asperity from kinematic source model of the 2013 Tohigi-ken hokubu, Japan, earthquake ( $M_w$  5.8) as a part of advanced characterized source modeling toward the prediction of strong motion.

The spatio-temporal stress change on the fault is calculated from kinematic source model using a three-dimensional finite difference method (FDM) for solving the elastodynamic equations (e.g., Ide and Takeo, *J. Geophys. Res.*, 102, 27379-27391, 1997). We employ the heterogeneous source model inverted from strong motion records in 0.1-1.0 Hz by Somei et al. (JpGU, SSS23-P19, 2014) as the kinematic source model input to FDM calculation. Each subfault size is divided into 250 x 250 m from 1.0 x 1.0 km, which is original size of inversion model, by bi-linear interpolating. We use the Staggered grid in FDM calculation. From the estimated stress change and slip amount, we extract the dynamic source parameters assuming the frictional constitutive law for each subfault.

The obtained dynamic source parameters are static and dynamic stress drops, effective stress, strength excess, critical slip-weakening distance ( $D_c$ ), and fracture energy ( $G_c$ ). We tried to evaluate the average value for each dynamic source parameters on and off the asperity, and to compare them for each other. The asperity area is defined as a rectangular area by characterizing the final slip on kinematic source model. The principal findings in this study are as follows: 1) The asperities have 2 times larger  $D_c$  than the off asperity area. 2)  $D_c$ 's on and off the asperities are about 50 % of the final slip amount. 3) Static and dynamic stress drops on the asperity are 3-5 times larger than those on the off asperity area. 4) Average static and dynamic stress drops, and effective stress on the asperity are 6.0, 6.7, and 7.7 MPa, respectively. 5) Strength excess tends to be large on the edge of the asperity.

**Acknowledgements:** This study was based on the 2015 research project 'Improvement for uncertainty of strong ground motion prediction' by the Nuclear Regulation Authority (NRA), Japan.

**Keywords:** The 2013 Tohigi-ken hokubu earthquake, Dynamic source parameter, Kinematic source model

## Slip velocity function for strong motion evaluation based on the hybrid method

\*Susumu Kurahashi<sup>1</sup>, Kunikazu Yoshida<sup>2</sup>, Ken MIYAKOSHI<sup>2</sup>, Kojiro Irikura<sup>1</sup>

1.Aichi Institute of Technology, 2.Geo-Research Institute

### 1. Introduction

Broad-band strong motion in general has been estimated by the hybrid method, long-period motions by a numerical method and short-period motions by a semi-empirical method. Ground motions from the long-period calculation and those from the short-period calculation are combined using matching filter about 1Hz. The synthesized waveforms by the hybrid method fit the observed records well in the previous researches (e.g. Kamae et al., 1998).

Slip velocity functions used above are different in the target frequency ranges. For example, smoothed ramp function, Nakamura and Miyatake's function (2000) and so on are used for the long period calculation. On the other hand, in case of the short-period calculation the slip time function is not directly defined but given as a convolution of the slip time function of small event with a correction function defined by Irikura (1986).

Therefore, the slip velocity function in intermediate period range from 0.5 to 1.0 s is expressed as the summation of the theoretical slip time function given in the long-period range and the empirical one in the short-period range.

However, there is a possibility that the combined spectra have some sag in the intermediate period range,

In this study, we discuss ground motion characteristics between the long-period waveform and short-period waveform in the intermediate period range during 2008 Iwate Miyagi Nairiku earthquake. First, strong motions generation area (SMGA) during this earthquake was estimated by the empirical Green's function method (Irikura, 1986). Second, theoretical long-period waveform was calculated by discrete wavenumber method (Bouchon, 1981) based on High Rate Area (HRA) characterized source model. We examine whether the both spectra of the synthesized waveforms are smoothly connected.

### 2. Estimation of Strong Motion Generation Area (SMGA)

SMGA source model during 2008 Iwate Miyagi Nairiku earthquake was already estimated by Kurahashi and Irikura (2013, 2014). We re-estimated the SMGA source model, because Yoshida et al. (2015) re-estimated the characterized source model which was constructed from slip distribution by the waveform inversion. Yoshida et al. (2015) proposed HRA characterized source model from peak moment rate distribution. Yoshida et al. (2015) thought that short-period strong motion is generated from HRA because short-period strong motion relates slip velocity function. Therefore, we re-estimated the SMGA source model by the empirical Green's function method (Irikura, 1986) referring to the HRA characterize source model. As a result, the synthesized waveform based on the HRA characterized source model agrees with the observed one.

Next, the long-period waveform was calculated by the discrete wavenumber method (Bouchon, 1981). Parameters of the slip time function were determined to comparison between the observed and synthesized waveform. We discuss how to select the slip velocity time function to smoothly connect between the long-period and short-period calculations.

Keywords: slip velocity function, the hybrid method, 2008 Iwate Miyagi nairiku earthquake

Study on spectral decay characteristics in high frequency range using parameter  $\kappa$ - For crustal earthquakes -

\*Masato Tsurugi<sup>1</sup>, Takao Kagawa<sup>2</sup>, Kojiro Irikura<sup>3</sup>

1.Geo-Research Institute, 2.Tottori University, 3.Aichi Institute of Technology

Spectral decay parameters  $\kappa$  and  $f_E$  due to crustal earthquakes are estimated in this study. In high frequency range spectra of S-wave accelerations are generally characterized by a trend of exponential decay,  $e^{-\pi f \kappa}$  ( $f > f_E$ ), while they are modeled with  $f_{max}$  filter in Japanese applications. The  $\kappa$ 's of the three large earthquakes are estimated in the range 0.0142 and 0.0277 and  $f_E$ 's are estimated in the range 2Hz and 5Hz for the mainshocks of the 2003 Miyagi-ken Hokubu earthquake, the 2005 Fukuoka-Ken Seiho-oki earthquake, and the 2008 Iwate Miyagi Nairiku earthquake. The relationship between  $\kappa$  and the power coefficient of  $f_{max}$  filter,  $s$ , and the relationship between  $f_E$  and  $f_{max}$  are evaluated from the results. Moreover, hypocentral distance dependency of  $\kappa$  is confirmed as demonstrated by previous studies.

Keywords: Spectral decay characteristics, Kappa, fmax filter, Crustal earthquakes

## Stochastic Green's Function Method Incorporated Empirical Site Effects in Time Domain

\*Takashi Akazawa<sup>1</sup>, Kojiro Irikura<sup>2</sup>

1.Geo-Research Institute, 2.Aichi Institute of Technology

Site effects make a great impact on ground motions on Earth's surface, in particular at places underlain by soft soils. For make an accurate estimation of ground motion, site effects need to be quantitatively evaluated in time domain, including phase information (hereinafter called the site effects as "non-stationary site effects"), although so far only amplitude spectra of the site effects are taken into account. Akazawa et al. (2009) developed a method for estimating the non-stationary site effects using the wavelet analysis and many seismic records. The method gives average amplitude property (envelope) depending on frequency and coherent phase of seismic records. Akazawa et al. (2009) showed the applicability of the method by demonstrating for the observed seismic records for small events.

We simulate observed seismic records for large events (e.g. the 2011 Tohoku Earthquake) by incorporating the non-stationary site effects, which was proposed by Akazawa et al. (2009), with the stochastic Green's function method. Bedrock ground motions from a small event are stochastically simulated with the omega-squared model and an envelope time function depending on source size and propagation path. Bedrock ground motions from a large event are evaluated taking fault model into account in the same procedure as the empirical Green's function. Surface ground motion from the large event is calculated with a convolution of the bedrock motion with the non-stationary site effects. This method applied to some large events whose source models are known. The simulated results agree well with the obtained seismic records.

Keywords: Site Effects, Time Domain, Stochastic Green's Function Method, Strong Ground Motion Method

## Broadband ground motion prediction considering variabilities of source parameters and comparison with observed records

\*Asako Iwaki<sup>1</sup>, Takahiro Maeda<sup>1</sup>, Nobuyuki Morikawa<sup>1</sup>, Hiroyuki Fujiwara<sup>1</sup>

1.National Research Institute for Earth Science and Disaster Prevention

The strong motion prediction "recipe" (Earthquake Research Committee, 2009) has proposed the characterized source model whose source parameters are determined by the scaling laws that extract average characteristics of the source parameters of past earthquakes. Consequently, the predicted ground motion of the National Seismic Hazard Maps using the characterized source models with a limited number of locations of the asperities and hypocenters may be at average level, which is insufficient for prediction of unknown earthquake ground motion. In order to overcome this problem, two approaches may be important. One is to comprehend the variabilities of the source parameters by analyzing the ground motion records of past earthquakes. The other is to introduce probabilistic source models and perform large amount of ground motion computation.

In this study, we attempt to perform "ground motion prediction" of past earthquakes by using source models that take into account the variabilities of source parameters. The 2000 western Tottori earthquake is chosen as our first target earthquake. Aleatory variabilities of selected source parameters are assumed to have normal distributions whose means and standard deviations are estimated from the recipe, and the source models are constructed by sampling the source parameters by the Latin Hypercube Sampling (LHS), following the method by Yamada et al. (2007, 2011).

Variabilities of five parameters are considered; the (1) short-period level (ratio to  $M_0^{1/3}$ ), (2) slip within the asperities (ratio to the average slip), (3) rupture velocity (ratio to the shear-wave velocity of the source region), (4) asperity locations, and (5) hypocenter location. As a preliminary analysis, we constructed source models in which the short-period level, asperity slip, and rupture velocity have either the mean or mean+SD values with fixed locations of asperities and hypocenter. Broadband ground motion was computed by a hybrid method of 3D FDM and the stochastic Green's function method. By comparing the simulation results with each other and with observation via an evaluation method using the 5% damped pseudo acceleration response spectra (PSA) at 40 stations with hypocentral distance of 1 -180 km (Goulet et al. 2015), we found that The basic case (all parameters have the mean values) over- and underestimated the PSA at long- (> 1 s) and short- (< 1 s) periods, respectively. The mean+SD short-period level amplified the PSAs at all stations at periods 1 s and shorter. The influence of the mean+SD rupture velocity model largely varied among the stations.

We will conduct ground motion simulations for ~100 source models in which all the five parameters are sampled by LHS. We will evaluate the variability of the predicted ground motions and compare them with the observed records. It is important to perform these analyses for various other past earthquakes in order to compare the variabilities of the predicted ground motions with those of the observed ground motions.

Keywords: ground motion prediction, source model, variability

## Introduction of rupture directivity effect into the pseudo point-source model

\*Yosuke Nagasaka<sup>1</sup>, Atsushi Nozu<sup>1</sup>

## 1. Port and Airport Research Institute

The pseudo point-source model (Nozu, 2012) is a simple source model for strong ground motion simulation. This simple source model has been applied to some earthquakes and shown good agreement with observations as well as the characterized source model.

In the pseudo point-source model, subevents which generate strong ground motions are assumed on the fault plane and a source spectrum which follows the omega-square model is given to each subevent. This means the spacio-temporal distribution of the slip within the subevent is not explicitly considered in the pseudo point-source model. Thus, parameters concerning rupture propagation such as the size of the subevent are not necessary. However, by giving a corner frequency properly the size of the subevents is implicitly taken into account.

A problem of the pseudo point-source model is that the rupture directivity effect is not considered. This is because we assume a source spectrum for each subevent without considering rupture propagation. As a result, the same source spectrum is used for forward and backward stations and underestimations can happen at stations where forward directivity is observed. In a previous study (Nagasaka et al., 2015) in which this model was applied to the 2005 Central Chiba earthquake ( $M_w$ 5.9), the results were generally good, however, underestimation was found in the west of the epicenter and this could be attributed to the fact that the current pseudo point-source model does not consider rupture directivity effect. To avoid such underestimation is important when this model is to be used for earthquake-resistant design.

In this study, in order to introduce rupture directivity effect into the pseudo point-source model, we investigated the applicability of a corner frequency model representing rupture directivity effect. The target is the 2005 Central Chiba earthquake ( $M_w$ 5.9). First, we searched for the optimal corner frequencies at each target station as the error between synthetic and observed Fourier spectra becomes minimum. The result was that the optimal corner frequency was about 1.0Hz in the west of the epicenter where underestimation was found in the previous study, in which the corner frequency of 0.75Hz was used for all the target stations. Therefore, this result indicates that forward directivity could have affected the stations to the west of the epicenter. The optimal corner frequencies were smaller at surrounding stations; this also implies that introducing rupture directivity effect can improve the pseudo point-source model.

Then, we assumed a unilateral rupture along a line source to model the corner frequency. Under this condition, the corner frequency becomes a function of the angle between the direction of rupture propagation and wave propagation to a target station ( $\phi$ ). New source parameters we need are the length of the rupture ( $L$ ), the rupture velocity ( $V_r$ ) and the direction of the rupture propagation. Then the corner frequency ( $f_c$ ) can be represented as  $f_c = (V_r / \pi L) (1 - V_r / V_s \cdot \cos\phi)$ . This means that the corner frequency varies depending on the apparent duration of the rupture; the corner frequency is higher in the forward region and lower in the backward region with respect to the rupture propagation. We plan to search for the parameters that minimize the error between the observed and synthetic Fourier spectra. Then, this result will be compared with the result of the previous study ( $f_c = 0.75\text{Hz}$ ). In addition, the rupture propagation indicated by the optimal parameters will be compared with the rupture process of the earthquake estimated from waveform inversion.

Keywords: strong ground motion simulation, pseudo point-source model, rupture directivity effect, corner frequency



## High Frequency Ground Motion Simulation of an Un-happened ShanChiao Fault in Northern Taiwan from an ETF-Based Site Correction Method for Stochastic Simulation

\*Jyun-Yan Huang<sup>1</sup>, Kuo-Liang Wen<sup>1,2</sup>, Che-Min Lin<sup>1</sup>, Chun-Hsiang Kuo<sup>1</sup>, Chun-Te Chen<sup>3</sup>, Shuen-Chiang Chang<sup>2</sup>

1.National Center on Research Earthquake Engineering, Taipei, Taiwan , 2.National Central University, Chung-Li, Taiwan, 3.Institute of Earth Science, Taipei, Taiwan

Strong motion generation area (SMGA) was mentioned as an important source parameter for high frequency strong motion simulation (Kurahashi and Irikura, 2011) that was identified as different asperity distribution from traditional source inversion results. Meanwhile, high frequency strong motion simulation is very important in application of engineering seismology. Site correction method from Empirical Transfer Function (ETF, Wen et al., 2013) for stochastic finite fault simulation was applied in Northwestern Taiwan for 1999 ChiChi Taiwan earthquake as high frequency simulation. Except the traditional inverted asperity model was used, random asperity distribution ones were test from Huang et al. (2014). In this study, different construction method of random asperity models followed Japan's Recipe (Irikura et al., 2004; NIED, 2009) are constructed for the same event first to check near fault response for randomly SMGAs. ShanChiao fault is the most important fault system in northern Taiwan owing to it could probably generate earthquake directly hit the Capital urban area. Finally, this study will try to identify possible ground shaking level for Shanchiao Fault system. The simulation results could help to preliminary plan of disaster prevention issue or building design problems in the future.

Keywords: Stochastic Simulation, Empirical Transfer Function, SMGA, ShanChiao Fault

## Simulation of long-period ground motions for the 2011 Tohoku earthquake (Mw9.0) using large-scale parallel computing

\*Kentaro Kasamatsu<sup>1</sup>, Kenichi Kato<sup>1</sup>

1.Kobori Research Complex INC.

In the 2011 off the Pacific coast of Tohoku Earthquake (Mw9.0), long-period earthquake ground motions were recorded all over Japan including KiK-net Konohana in Osaka. It is important to clarify the reproducibility and the propagation characteristics of long-period ground motions to improve the S-wave velocity model of deep sedimentary layers and predict ground motions of the large earthquake occur in Nankai troughs. To simulate the earthquake ground motion for all over Japan, we developed a parallel computing program using 3D finite difference method based on domain decomposition. We simulated the earthquake ground motions of the March 11 main shock using the developed program, and examined the reproducibility of earthquake ground motions at periods from 2 to 10s in the Metropolitan area.

For effective parallel calculations of earthquake ground motions using 3D finite difference method, we deployed 3 computers equipped with 2 CPUs made by Intel (E5-2690v3, 12 cores) and memory cards of 192Gbyte in each node. We connected 3 nodes using the InfiniBand of 40Gbps transmission speed and constructed the calculation environment that enabled 72 parallel computing with inter-node communication using MPI. The parallel calculation was based on the 3D domain decomposition to utilize a large number of cores which were equipped in each node effectively, and used MPI in intra-node communication as well. We checked the parallel efficiency by simple examples. Scalability was approximately 15 times in case of 32 processes. When we used another PC cluster (16 nodes, 2 CPUs, 8 cores), scalability was approximately 60 times in case of 64 processes. Overall execution time was shortened approximately as expected.

We simulated long-period earthquake ground motions of the March 11 main shock using pseudo point-source model (Nozu, 2012) for the purpose of examining the applicability of point-source at periods from 2 to 10s. Source time functions were triangle type and the number of time window was 1. Dip angle was 90 degrees for all point-sources. Rise times were set based on the corner frequencies of Nozu (2012). We used S-wave velocity model of deep sedimentary layers of Headquarters for Earthquake Research Promotion (2012). The calculational domain was East-West 300km, North-South 600km, and vertical 100km. We digitized the model with grid of 0.2km for horizontal and 0.1km to 1.0km for vertical. Total number of grids was approximately 1,600 million, and duration time was set to 300s with the time interval of 0.005s. We finished calculation of 60001 steps in less than two days. When we compared observed and simulated earthquake ground motions at periods from 2 to 10s, shapes of the spectra were well reproduced although amplitudes at periods from 6 to 10s were underestimated in the metropolitan area likely due to the point-source modeling. Surface waves (T=6-10s) generated around south of Ibaraki Prefecture propagated toward the metropolitan area were almost reproduced except for amplitude. Continuously, we are going to adjust the source model of the March 11 main shock, and investigate the propagation characteristics of long-period ground motions. In addition, we will implement the developed program in the Earth Simulator.

Keywords: parallel computing, finite difference method, the 2011 off the Pacific coast of Tohoku Earthquake, long-period ground motion

## Benchmark Test for Strong Motion Simulation in The Tokyo Metropolitan Area.

\*ayato ishikawa<sup>1</sup>, Yoshiaki Hisada<sup>2</sup>

1.Graduate school , Kogakuin University, 2.Kogakuin University

We conducted a benchmark tests for strong motion simulation methods .

we simulated the long-period ground motions in the Kanto sedimentary basin using the 2005 northwestern Chiba earthquake (M6.0) , and using the supposed Tokyo metropolitan earthquake in STEP8.

Keywords: Strong ground motion prediction, Benchmark test

## A New Attenuation Relationship for Velocity Response Spectra at the surface

\*Akemi Noda<sup>1</sup>, Ritsuko S. Matsu'ura<sup>2</sup>, Mitsuko Furumura<sup>2</sup>, Hiroto Tanaka<sup>1</sup>, Tsutomu Takahama<sup>1</sup>

1.Kozo Keikaku Engineering Inc., 2.Earthquake Earthquake Research Center, Association for the Development of Earthquake Prediction

We integrated the attenuation relationships proposed by Matsu'ura et al.(2011) to be able to predict the velocity response spectrum for an arbitrary source at an arbitrary site in wide range of distance and period. We divided data into three groups of source types as follows: inter-plate, intra-plate, and very shallow earthquakes. In order to determine parameters at once, we expand each parameter by cubic B-splines, as Yabuki and Matsu'ura(1992) did, and transform the problem to be solved in a linear inversion. We also introduce the upper limit of the plate depth at a site to be considered, such as 250km for PAC slab, by comparing AICs for various limit depth and various types of formulae.

$Sv_{ij}$  is the velocity spectrum at the  $i$ -th site of hypocentral distance  $DELTA_{ij}$ , where the depth of subducting slab is  $dep_i$ , due to the  $j$ -th earthquake of  $Mw_j$  with the residual of  $e_{ij}$ . For inter-, and intra-plate earthquakes, the relation is the form of Eq. (1), while for very shallow earthquakes, Eq. (2) is the form. Here,  $t$  is the period.

$$\log Sv_{ij}(Mw_j, DELTA_{ij}, dep_i, t) = Mw_j A_w(t) + A_c(t) - Beta(t) \log(DELTA_{ij}) - d(t) dep_i + e_{ij}(t) \text{ Eq.(1)}$$

$$\log Sv_{ij}(Mw_j, DELTA_{ij}, t) = Mw_j A_w(t) + A_c(t) - b(t) DELTA_{ij} - Beta(t) \log(DELTA_{ij}) + e_{ij}(t) \text{ Eq.(2)}$$

In Eq. (1), the term with the coefficient  $b(t)$ , which is always contained in conventional engineering formulae of the attenuation relationship for response spectra, is omitted. We found: 1) the term with  $b(t)$  in Eq. (2) works to represent the plateau shape of spectra in very small  $DELTA$ , especially in short period. 2) The coefficient  $Beta(t)$ , which we introduced, works well alone to fit data of inter- and intra-plate earthquakes without  $b(t)$ , since data with very small  $DELTA$  are rare for those types of earthquakes in Japan. 3) Even in Eq. (2),  $b(t)$  is nearly zero for periods over about 2sec. 4) The coefficient  $d(t)$  in Eq. (1), which is usually believed to represent the effect of High-Q and High-V subducting slab, is even effective to represent the effects from large scale of geological structure differences in Japanese crust, such as rather low Q features of western part of the northeastern Japan, and the attenuation discrepancy between the east and west of the Hida mountains.

The site response  $e_{ij}(t)$  is almost independent of the source types,  $Mw_j$ , and  $DELTA_{ij}$ , i.e. nearly equal to  $e_i(t)$ . It was empirically confirmed that  $e_i(t)$  can be replaced by H/V spectral ratio obtained from the observed micro-tremors. Eqs. (1) and (2) can be used to calculate velocity spectra at any site for any expected sources without knowing AVS30 or geotechnical classification of that site.

This study was done by the trust from Ministry of Education, Culture, Sports, Science and Technology.

Keywords: Attenuation relationships of Velocity Response Spectra, Upper limit of the effective plate depth at a site, Selection by AIC, linear inversion method with cubic B-spline expansion

## Validation of Attenuation Relationships for Velocity Response Spectra, Comparing with Observed Records

\*Hiroto Tanaka<sup>1</sup>, Akemi Noda<sup>1</sup>, Tsutomu Takahama<sup>1</sup>, Mitsuko Furumura<sup>2</sup>, Ritsuko S. Matsu'ura<sup>2</sup>

1.Kozo Keikaku Engineering Inc., 2.Research Division, Earthquake Research Center, Association for the Development of Earthquake Prediction

An attenuation relationship for velocity response spectra has been proposed for wide range of period and distance by Noda *et al.* (2016), which is referred to as N2016 model hereafter. The optimum functional form of attenuation relationship was determined from observed records by using AIC. In this study, in order to validate the obtained relationship, we compare its result with observed one or with other previous studies.

For the comparison, we select two inter-plate earthquakes (the 2003 Tokachi-oki and the 2011 Tohoku-oki), three intra-plate earthquakes (the 2003 Miyagi-oki, the 2004 off the Kii peninsula, and the 2011 Miyagi-oki), and three crustal earthquakes (the 2000 Western Tottori, the 2005 west off Fukuoka, and the 2008 Iwate-Miyagi Nairiku). These events have magnitude larger than Mw6.6, and we can use a lot of observed records from K-NET and KiK-net. As previous studies, we select attenuation relationships obtained by Uchiyama and Midorikawa (2006), Satoh (2008, 2010), and Morikawa and Fujiwara (2013). Since these previous models are constructed for acceleration response spectra, we transform predicted amplitudes calculated from the previous models into pseudo-velocity response spectra. We calculate velocity or pseudo-velocity response spectra at free surface by multiplication of site amplification factors revealed by each researcher, and then compare them with observed velocity response spectra, for period ranging from 0.1 to 5 sec, within applicable range of each model.

The spectral amplitudes predicted by N2016 model agree well with the observation over a wide range of distances, up to farther than 200km. Furthermore, the dispersion of residuals between the predicted and observed amplitudes is very small over a wide range of periods, from 0.1 to 5sec. On the other hand, though the previous models explain well short-period components of the observed response spectra for distances shorter than about 150 km, the dispersion of residuals between observed and their predicted amplitudes increases with distance. The good agreement between observation and N2016 model is mainly for two reasons: (1) effectivity of attenuation terms proportional to depth of subducting slab, (2) regarding coefficients of attenuation terms proportional to logarithm of distance as unknown quantities for each period. The latter suggests that we cannot assume a priori that the coefficients are 1.0 in the Japan Islands. We can attribute the small dispersion of N2016 model to effectivity of site amplification terms, which is obtained from residuals for each period, at each station.

This study was made by the trust from Ministry of Education, Culture, Sports, Science and Technology.

### References

- Morikawa, N. and H. Fujiwara, 2013, A new ground motion prediction equation for Japan applicable up to M9 mega-earthquake, *Journal of Disaster Research*, 8, 878-888.
- Noda, A., Matsu'ura, R. S., Furumura, M., Tanaka, H. and Takahama. T., 2016, A new attenuation relationship for velocity response spectra at the surface, JPGU Meeting 2016.
- Satoh, T., 2008, Attenuation relations of horizontal and vertical ground motions for P wave, S wave and all duration of crustal earthquakes, *J. Struct. Constr. Eng., AIJ*, 632, 1745-1754. In Japanese with English abstract.
- Satoh, T., 2010, Attenuation relations of horizontal and vertical ground motions for intraslab and

interpolate earthquakes in Japan, J. Struct. Constr. Eng., AIJ, 647, 67-76. In Japanese with English abstract.

Uchiyama, Y. and Midorikawa, S., 2006, Attenuation relationship for response spectra on engineering bed rock considering effects of focal depth, J. Struct. Constr. Eng., AIJ, 606, 81-88. In Japanese with English abstract.

Keywords: attenuation relationship, velocity response spectra

## Probabilistic Seismic Hazard in Low Seismicity Region: Kalimantan, Indonesia

\*Sri Hidayati<sup>1</sup>, Athanasius Cipta<sup>2</sup>, Amalfi Omang<sup>1</sup>

1.Center for volcanology and Geological Hazard Mitigation, 2.Australian National University

The island of Kalimantan lies upon the southeastern margin of the greater Eurasian plate. The features that affected Kalimantan came from its great tectonic activity during Late Paleozoic-Pliocene. The absence of present-day major earthquakes makes the island is considered as a relatively stable block. In the past decades, seismic hazard analysis in Kalimantan is not prioritized due to its low seismicity. However, two moderate yet destructive earthquakes hit the island in 2015: the 6.5 Mw Sabah (Northern part of Kalimantan, Malaysia) earthquake on June 5, and the 6.1 Mw Tarakan (Eastern part of Kalimantan, Indonesia) earthquake on December 21. It seems that the eastern and northern parts of the island are subject to potential hazard from small to medium sized earthquakes. Those recent earthquakes show that Kalimantan is not sterile from destructive earthquakes. Hence, we must remain alert to the possibility of such an earthquake disaster, as it had happened last year and 95 years ago. In addition, more than 18 million people living in this island should be considered.

In order to reduce earthquake disaster, the Kalimantan seismic hazard map was created using probabilistic approach called PSHA. The uncertainties of size, location and time of earthquake sources and GMPE were taken into account in calculation of acceleration. Seismic hazard analyses involve the quantitative estimation of ground-shaking intensity that was obtained by converting the acceleration on 0.3 second RSA (Response Spectral Acceleration) having 10% probability of exceedance in 50 years (500 years return period). Based on ground-shaking intensity, the hazard level was divided into four classes: they are very low ( $MMI < V$ ), low ( $V \leq MMI \leq VII$ ), moderate ( $VII < MMI \leq VIII$ ), and high ( $MMI > VIII$ ) respectively. Important to note, this classification is primarily intended to non-engineered building, a common building in Indonesia.

The hazard level in Kalimantan is mainly controlled by diffuse zones of deformation (background seismicity) while Palu Koro and/or North Sulawesi subduction affected eastern tip of Mangkalihat Peninsula. The inclusion of site amplification is another important aspect that included in the hazard map, since it can change the hazard level significantly.

Keywords: PSHA, Kalimantan , Low Seismicity Region, Seismic Hazard Map

## The Impact of Westward Extension of Flores Back-Arc and The Inclusion of an Active Crustal Fault in Southeastern Bali to Bali Seismic Hazard Map (Preliminary Results)

\*Amalfi Omang<sup>1</sup>, Sri Hidayati<sup>1</sup>, Irwan Meilano<sup>2</sup>, Asdani Soehaimi<sup>3</sup>

1.Center for Volcanology and Geological Hazard Mitigation, Indonesian Geological Agency,

2.Institute of Technology Bandung, 3.Center for Geological Survey, Indonesian Geological Agency

Recent study utilising Global Positioning System (GPS) measurements of surface deformation conducted in western area of Lesser Sunda Islands, show the westward extension of Flores Back-Arc for 300 km onshore into East Java. Another recent study, utilising geology, geophysics and geodetic methods reveal indication of an active crustal fault in southeastern Bali which pass Denpasar, the capital city of Bali Province and the most dense city in its province. The Implications of these findings are the increasing hazard and risk levels in Northern and Southeastern parts of Bali. Seismic hazard analyses (deterministic and probabilistic) using OpenQuake show increasing hazard levels compared to the previous seismic hazard map of Bali. The direct impacts are the number of people and buildings affected by the inclusion of these seismic sources increase significantly. The preliminary results show the need for a careful evaluation of the infrastructures and contingency plan within areas which affected by these seismic sources in order to ensure the safety of the people and to reduce loss of infrastructures.

Keywords: Back-Arc, Active crustal Fault, Seismic Hazard Analyses, OpenQuake

## A proposal for creating a maximum seismic intensity map of past damaging earthquakes

\*Reiji Kobayashi<sup>1</sup>, Koichi Nakamoto<sup>2</sup>

1.Graduate School of Science and Engineering, Kagoshima University, 2.Faculty of Science, Kagoshima University

The Headquarters for Earthquake Research Promotion of Japan has created and published national seismic hazard maps, in principle, every year after the 1995 Hyogo-ken Nanbu earthquake. This hazard map has two problems. One is that probabilities cannot be easily understood by citizens. The other is that the method includes large uncertainties and has not been inadequately tested yet. The results, therefore, are less reliable.

We propose creating a maximum seismic intensity distribution of past damaging earthquakes. This maps may be easily understood by citizens, the method has small uncertainties and the result is more reliable. The distribution is two-dimensional and is enable citizens to know the maximum seismic intensity at their own backyard. The previous seismic intensity maps for historical earthquakes show the intensity only at the observation point, and the citizens cannot know the intensity at their own backyard.

Citizens in areas of large intensities may have a conscious to earthquakes. However, we should inform citizens in areas of small intensities that the area may not be safe in the future. It is preferable that this maps is supplementally used.

This study develops a map in Kumamoto prefecture for damaging earthquakes after the Meiji era as a prototype. We applied attenuation relationships for seismic intensity (Morikawa et al., 2010). We use fault planes if faults is estimated or hypocenters if the fault plane is not estimated to calculate distances in the equation. We also use the elevation data of the National Land Numerical Information download service to calculate distances. We use data of average shear-wave velocity in the upper 30 m distributed by the Japan Seismic Hazard Information Station. We estimate seismic intensity at each block of 250 m mesh for each earthquake and plot the maximum intensity at each block.

Seismic intensity of 4 (in JMA scale) are distributed in the most of Kumamoto prefecture due to the 1946 Nankai (M8.0) and 1968 Hyuganada (M7.5) earthquakes. High intensity (5 lower-6 higher) are distributed around Kumamoto city due to the 1889 Kumamoto earthquake (M6.3).

Keywords: seismic intensity, disaster prevention

## Amplification characteristics in Kanto district estimated from waveforms of the 2015 Ogasawara Deep earthquake with Mw8.0

Naoki Ueta<sup>1</sup>, \*Takuji Yamada<sup>2</sup>, Jun Kawahara<sup>2</sup>

1.College of Science, Ibaraki University, 2.Faculty of Science, Ibaraki University

A deep large earthquake with Mw8.0 took place beneath the Ogasawara islands on May 30, 2015. This earthquake caused a large shaking in Kanto district in Japan with the JMA intensity of 4 to 5 major, which provides an opportunity to investigate the amplification characteristics in the region.

We analyzed waveforms of 56 KiK-net sites in Kanto district and investigated the spectral ratio of the observed waveforms at stations on the surface and on the bedrock in the borehole at each site. We first picked arrival times of P and S waves and cut the waveforms from -10.00 to 30.95 s after the arrivals. We then calculated spectra of the waveforms and obtained the spectral ratios of P and S waves. We calculated average values of spectral ratios in the frequency band from 0.1 to 1 Hz (Fig. 1a) and attributed them to amplification factors at each KiK-net station.

We first investigated the relationship between the observed amplification factors and distances of surface and borehole seismometers. The relationship showed a good proportionality with a correlation coefficient of 0.744, indicating that the factors have a strong correlation with the thickness of the sediments the same as results of previous studies. We then calculated the normalized amplification factors (NA factors) for every 100 m of the distance between surface and bedrock stations to remove the effect associated with different thickness of sediment at each site (Fig. 1b). The NA factors were around 1 for sites at mountain regions as expected. In the Kanto plain, only sites around the Tone river had high NA factors.

Acknowledgements: We used KiK-net waveform data.

Keywords: Spectral ratio, KiK-net, Kanto district

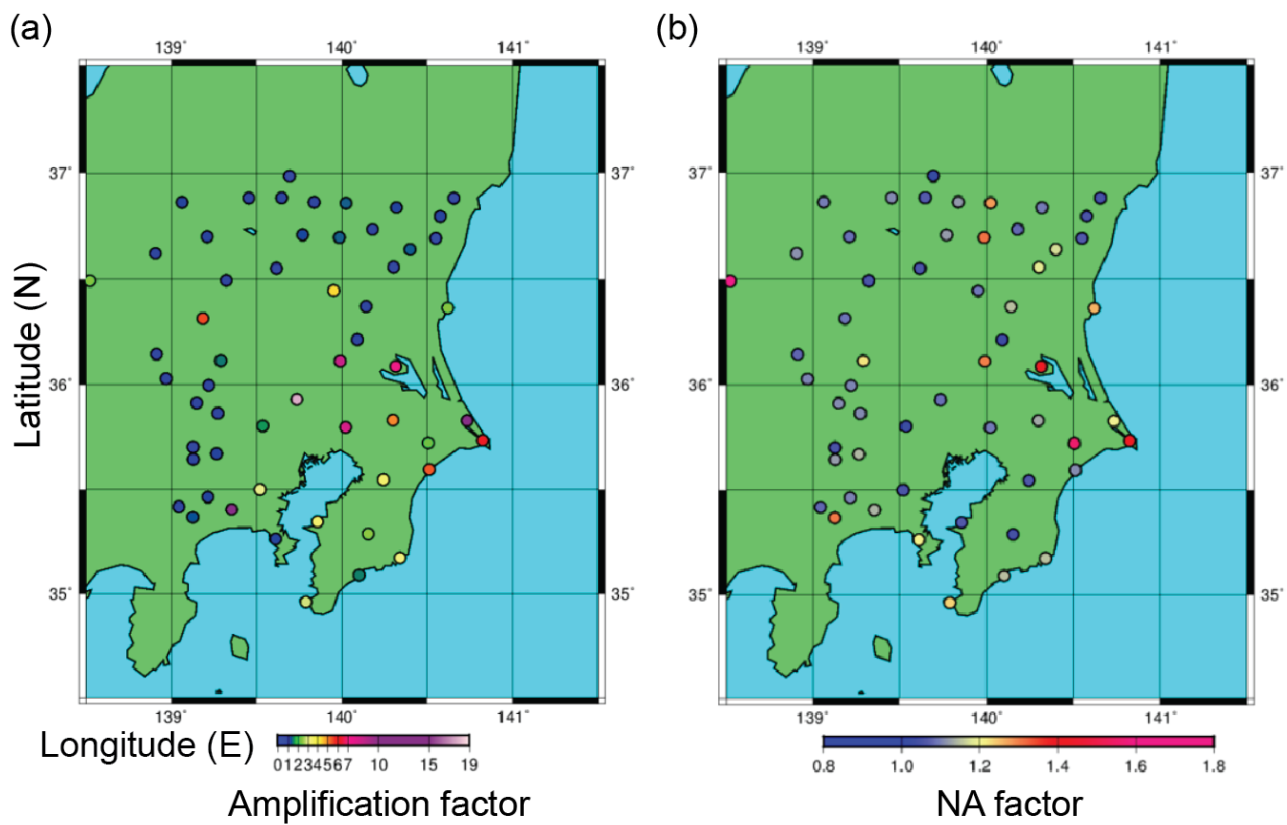


Fig. 1 (a) Amplification factors at KiK-net sites. (b) Normalized amplification factors.

## Variations in strength and predominant period of long-period ground motions around the northern Kanto sedimentary basin due to epicentral directions

\*Kengo Kajikawa<sup>1</sup>, Kazuo Yoshimoto<sup>1</sup>, Shunsuke Takemura<sup>2</sup>

1.Yokohama City University, 2.National Research Institute for Earth Science and Disaster Prevention

### Introduction

In the Kanto sedimentary basin, long-period ground motions are frequently observed and those predominant periods are affected by the bedrock depth of sedimentary basin (e.g., Yoshimoto and Takemura, 2014). Furthermore, excitation of long-period ground motions varies by epicentral directions of earthquakes (e.g., Yuzawa and Nagumo, 2012). In spite of these observational findings, less well known are the excitation characteristics of Love and Rayleigh waves, which cause long-period ground motions in the basin. Thus, in this study, we analyzed horizontal and vertical waveforms collected from stations of K-NET, KiK-net, and SK-net to investigate the characteristics of strength and predominant period of long-period ground motions during earthquakes with different epicentral directions.

### Analyzed earthquakes and analytic method

We analyzed eight shallow moderate-to-large earthquakes (Mw 5.8–6.9) having a wide coverage of epicentral directions. The CMT solutions of these earthquakes by F-net indicated that hypocentral depths were shallower than 8 km and source mechanisms were reverse or normal fault types. To analyze long-period ground motions which appeared after the arrival of S waves, we selected waveforms using the following recording conditions: a) at epicentral distances shorter than 150 km, waveforms recorded at least 100 s from earthquake origin time; b) at epicentral distances longer than 150 km, waveforms recorded over 150 s in total length or 200 s from earthquake origin time. We calculated Fourier spectra of velocity waveforms to investigate strength and predominant period of long-period ground motions observed in the Kanto basin.

### Variations of long-period ground motions due to epicentral directions

Comparison between horizontal- and vertical-component Fourier spectra revealed that, for all earthquakes, the magnitude of horizontal amplitude spectra dominated over that of vertical amplitude spectra, and horizontal predominant period was longer than vertical one, suggesting the dominance of Love waves over Rayleigh waves in the Kanto sedimentary basin. As for the predominant period, clear bedrock depth changes were observed for both components: the deeper bedrock depth, the longer predominant period. In a strict sense, this relationship held only in the area where the bedrock depth was shallower than 2 km, but otherwise the predominant period became almost constant values (Horizontal: 6.3 s, Vertical: 4.8 s) in deep (> 2 km) bedrock area. These observations were also consistently explained by assuming the dominance of Love waves over Rayleigh waves.

Analysis of the amplitude and the predominant period of long-period ground motions during The Mid Niigata prefecture Earthquake in 2004 (NW event) and the earthquake in Hamadori region of Fukushima prefecture on April 11, 2011 (NE event) revealed that the observed spectral amplitudes were almost the same for these earthquakes but the predominant periods were clearly different between these earthquakes: predominant periods of horizontal- and vertical-component observed at deep (> 2 km) bedrock area were approximately 6.6 s and 5.2 s, respectively, for NW event, and were 5.6 s and 4.6 s, respectively, for NE event. This observation suggested that the excitation of both horizontal and vertical long-period ground motions was affected by the difference in epicentral directions.

### Acknowledgement

The K-NET/KiK-net waveform data and the F-net CMT solution data were provided by the National Research Institute for Earth Science and Disaster Prevention, Japan. SK-net waveform data were

provided by the Earthquake Research Institute at the University of Tokyo.

Keywords: long-period ground motion, Kanto sedimentary basin, variation due to epicentral direction, predominant period, surface wave

## Source Azimuthal Dependence of Long-Period Ground Motions in the Kanto Basin and the transition of time-history

\*Masanori Noyori<sup>1</sup>, Seiji Tsuno<sup>2</sup>, Hiroaki Yamanaka<sup>3</sup>, Kosuke Chimoto<sup>3</sup>

1.Tokyo Institute of Technology (Former), 2.Railway Technical Research Institute, 3.Tokyo Institute of Technology

During the 2011 off the Pacific coast of Tohoku Earthquake, long-period ground motions were observed in the Kanto basin; therefore, long-period structures located in the Kanto basin were largely shook. Some articles (e.g. Yuzawa and Nagumo, 2012; Tsuno et al., 2012) pointed out that amplifications of long-period ground motions observed in the Kanto basin have the source azimuthal dependence by the data analyses on the main shock and aftershocks. Tsuno et al. (2012) reported that long-period ground motions whose periods were larger than 3 seconds has the characteristics of source azimuthal dependence, using the ratio of the pseudo-velocity response spectrum on surface to that at borehole.

We have investigated the source azimuthal dependence in the Kanto Basin, by data of the observations and the simulations for 10 earthquakes occurred around the Kanto Basin (Noyori et al., 2015). As a result, we could confirmed the same tendency between the observations and the simulations that long-period ground motions larger than 3 seconds were largely amplified for earthquake located in in north-west (Niigata pref.) direction and south-west (Shizuoka pref.) direction. In this study, we investigated the transition of source azimuthal dependence in the time history, which are related to the propagation of seismic motions in the Kanto basin.

Keywords: Long-period ground motion, Source azimuth, Site effect, Kanto Basin

## Equivalent-Linear Site Response Analysis in the Kanto Plain

\*Rami Ibrahim<sup>1</sup>, Tetsu Masuda<sup>1</sup>, Kazuki Koketsu<sup>1</sup>, Takeshi Hirose<sup>2</sup>, Hideaki Takaku<sup>2</sup>

1.Earthq. Res. Inst., Univ. Tokyo, 2.East Nippon Expressway Company Limited

The Kanto plain, the largest and most populated plain in Japan, is covered with thick marine sediments that can cause large amplifications of seismic waves during a big earthquake. The sediments thickness over the engineering base reaches to several hundred meters under the central part of Tokyo Metropolitan area. In this study, we evaluated the nonlinear site responses of layers between engineering base and free surface in the Kanto plain. We adopted an equivalent linear approach using DYNEQ program developed by Yoshida and Suetomi (1996) for the site response analyses. We use stochastic Green's function method to generate synthetic waveforms from 16 hypothetical earthquake source models located in the crust, and on the interface or within the of subducting Philippine Sea Plate. The simulations were done between the seismic sources and the engineering base where shear-wave velocity is equal to 500 m/s. Synthetic waveforms on the engineering base were used as input motion in DYNEQ program. Shear modulus versus strain ( $G/G_0-\gamma$ ) and damping versus strain ( $h-\gamma$ ) relationships of Central Disaster Management Council of Japan (CAO) are recognized to express the dynamic shear deformation of soil (clay, sand, and gravel). Shallow shear-wave velocity structural models above the engineering base were also provided by CAO. Resultant waveforms on the free surface show a systematic dependence on the thickness of soft structures above the engineering base. Large amplifications are dominant at short periods above shallow soft sediments, whereas peak amplitudes shifted to longer periods for sites located above deep soft sediments. Nonlinear site effects, inferred by de-amplification of the site responses, were typically obvious at short periods of approximately 0.2 s and shorter. Predominant periods of the soil was calculated based on empirical relations and compared to those obtained from the spectral ratio. Both predominate periods show disagreement at sites where nonlinear site responses are expected. The large deformations are mostly concentrated in shallow 30 m of soil inferred from shear strain analysis. Our analyses showed considerable effects of nonlinear response of surface layers to large seismic inputs on the engineering base. Our results reconfirm the importance of nonlinear soil effect consideration in risk assessment of structures.

Keywords: Equivalent linear approach, Site effects, Tokyo Meteropolitan Area

## The Effects of Thick Sediments to Long-period Ground Motion in Northern China

\*Yiqiong Li<sup>1</sup>

1. Institute of Geophysics, China Earthquake Administration, Beijing, China

The study of ground motion is a cross research field between earth science and engineering science. Theoretical seismologists are more concerned about propagation path and the effect of seismic focus, while engineering seismologists are more concerned with the ground effect. Studies have shown that the western Taiwan coastal plain is influenced by long-period ground motion from the 1999 Chi-Chi, Taiwan, earthquake, and engineering structures with natural vibration long-period are damaged by strong surface wave in the western coastal plain. The thick sediments in the western coastal plain are the main cause of the propagation of strong long-period ground motion. The thick sediments similar to in the western coastal plain also exist in northern China.

It is necessary to research the effects of thick sediments to long-period ground motion in northern China. The numerical simulation of ground motion based on theoretical seismology is one of important means to study the ground motion. We will carry out the numerical simulation of long-period ground motion in northern China by using the existing tomographic imaging results of northern China to build underground medium model, and adopting finite fault source model for wave input. In the process of simulation, our previous developed structure-preserving algorithm, symplectic discrete singular convolution differentiator (SDSCD), is used to deal with seismic wave field propagation. Our purpose is to reveal the formation and propagation of long-period surface wave in thick sediments and grasp the amplification effect of long-period ground motion due to the thick sediments. It will lay the foundation on providing the reference for the value of the long-period spectrum during determining the ground motion parameters in seismic design. This work has been supported by the National Natural Science Foundation of China (Grant No.41204046, 42574051).

Keywords: Thick Sediments, Long-period Ground Motion

## A multi-period inversion of broadband seismic waveforms for 3-D velocity structures

\*Yujia Guo<sup>1</sup>, Kazuki Koketsu<sup>1</sup>

1. Earthquake Research Institute, University of Tokyo

A precise velocity structure model is necessary to predict long-period ground motions during large earthquakes and analyze source processes using long-period waves. Many studies have reported that 3-D velocity structures formed by sedimentary basins or accretionary wedges along subduction zones can significantly affect the generation and propagation of long-period seismic waves. In terms of including the various effects of the 3-D velocity structures, a waveform inversion for 3-D velocity structures using the time history of long-period ground motions is the most effective. These were several studies that estimated 3-D velocity structures by waveform inversions. Aoi (2002) proposed a method that estimates the 3-D depth of the boundary between sediment and bedrock. Iwaki and Iwata (2011) applied the method of Aoi (2002) to real data observed in the Osaka basin, Japan. Hikima (2006) formulated an inversion procedure for 3-D velocity structures, in which observed waveforms are initially inverted for layer thicknesses in 2-D cross-sections and a 3-D velocity structure model is subsequently constructed by interpolating the results of the 2-D inversions. In southern California, the estimations of the seismic velocity and the intrinsic attenuation were performed by the numerical simulations of wave propagation in combination with the adjoint method (e.g., Askan and Bielak, 2008; Tape *et al.*, 2010).

Seismic waveforms with a period range such as 2-20 s are often used to evaluate long-period ground motions. Thus, it is important to construct a velocity structure model which well reproduces the waveforms filtered over this period range. In this study, we attempt to develop a waveform inversion method for 3-D velocity structures that are responsible for broad-period ground motions. We first divide the inverted period range into multiple period ranges such as 10-20, 5-20, and 2-20 s. We start our inversion with the waveforms with only the longer-period range (10-20 s). The solution for the current period range is used as an initial guess for the next period range, which includes the shorter period (5-20 s). The inversion is continued until the period range matches the broadest period (2-20 s). The velocity structure model is composed of homogeneous layers, and the layer thicknesses are set as model parameters, just as Hikima (2006) did. The model parameters are estimated by solving a non-linear damped least-squares problem, which is an iterative procedure. In the inversion using only longer-period waveforms (10-20 and 5-20 s), we can use coarse inversion grids (e.g., Bunks *et al.*, 1995); in the inversion using the waveforms with the broadest period (2-20 s), a reasonable initial guess leads the iteration to achieve a fast convergence. Thus, our inversion procedure is better than conventional waveform inversions in terms of reducing the total number of 3-D forward simulations. Furthermore, we can stably estimate the model parameters for a complex velocity structure with multiple layers.

We calculate the partial derivatives with respect to model parameters using finite-difference approximation, where the difference between the unperturbed and slightly perturbed synthetic waveforms is taken. The synthetic waveforms are calculated by a 3-D finite element method with voxel meshes (Koketsu *et al.*, 2004; Ikegami *et al.*, 2008). We also use the modified Levenberg-Marquardt method to make the iteration stable. At each iteration, the model parameters are solved by the singular value decomposition of the Jacobian matrix. We performed several numerical experiments to confirm the validity of our inversion procedure. We will show the results and discuss the performance of the recovery of broad-period data as well as the optimal way to divide the inverted period range.

Keywords: Velocity structure model, Waveform inversion, Broadband seismic waveform, Damped least-squares method, Non-linear problem

## Performance Check of the Velocity Structure Model of Oita Prefecture Using Strong Motion H/V and R/V Spectral Ratio

\*Masayuki Yoshimi<sup>1</sup>, Masayuki Yamada<sup>2</sup>

1.Geological Survey of Japan, AIST, 2.NEWJEC Inc.

S-wave velocity structure of Oita prefecture is checked using H/V and R/V spectral ratio analyzed with strong motion data observed with strong motion network operated by Oita Prefecture. See detail in our Japanese abstract.

Acknowledgement: This research has been done under the Comprehensive Research on the Beppu-Haneyama Fault Zone (FY 2014-2016) by MEXT, Japan. Strong motion data are provided by Oita Prefecture and NIED.

Keywords: H/V spectral ratio, R/V spectral ratio, three-dimensional velocity structure model

## Estimation of Subsurface Structure Using Receiver Function at Seismograph Observatory Site in Tottori Prefecture

\*Tatsuya Noguchi<sup>1</sup>, Hayato Nishikawa<sup>2</sup>, Shohei Yoshida<sup>1</sup>, Takao Kagawa<sup>1</sup>

1.Department of Management of Social Systems and Civil Engineering, Civil Engineering Course Graduate School of Engineering, Tottori University, 2.National Institute of Technology, Maizuru College

In this study, subsurface structures of strong ground motion observation sites in Tottori Prefecture were estimated from receiver functions at seismograph observatory sites. PS-P times were obtained from receiver functions of observation data and parameter of existing underground model (J-SHIS model etc.). The PS-P times were compared with both results at each site and subsurface structure models were estimated by adjusting the layer thickness of initial model. Theoretical receiver functions were calculated from subsurface structure by using Haskell matrix and subsurface structure models were estimated by comparison of both receiver function.

Keywords: Receiver function, Subsurface structure, Seismograph observatory site, Tottori Prefecture

## Exploration of Underground Structure and Analysis of Seismic data in Central Area of Tottori Prefecture

\*Tatsuya Noguchi<sup>1</sup>, Hiroshi Ueno<sup>1</sup>, Sho Nakai<sup>1</sup>, Shoya Arimura<sup>1</sup>, Kazu Yoshimi<sup>1</sup>, Takao Kagawa<sup>1</sup>, Shohei Yoshida<sup>1</sup>

1.Department of Management of Social Systems and Civil Engineering, Civil Engineering Course  
Graduate School of Engineering, Tottori University

An earthquake (in 1983, M6.2) which caused disasters in Kurayoshi City occurred in central area of Tottori Prefecture. In this study, microtremor and gravity survey were carried out to estimate underground structures in the target area. Furthermore, aftershocks were observed at temporary seismic observatories around focal region and the seismic data (include data of municipalities) were analyzed. S-wave velocity model, microtremor H/V spectrum and a gravity basement structure were obtained from underground explorations. Characteristics of seismic indexes of target observatories were understood from analysis of seismic data.

Keywords: Underground structure, Geophysical exploration, Seismic data, Central Area of Tottori Prefecture

## Estimation of Rayleigh Wave Phase Velocities around the Beppu Bay Area using Long-period Volcanic Signals

\*Takumi Hayashida<sup>1</sup>, Masayuki Yoshimi<sup>2</sup>

1.IISEE, Building Research Institute, 2.Geological Survey of Japan, AIST

We deployed a dense seismic array consisting of 12 broadband stations after late August 2014 around the Beppu bay area, Oita prefecture to investigate seismic velocity structure of deep sedimentary basin (Hayashida et al., 2015, JpGU Meeting). Around the same time of the installation, long-period volcanic tremors at Aso volcano (Kaneshima et al., 1996, Science) have been frequently generated [e.g. Sandanbata et al. (2015, JpGU Meeting); Matsuzawa et al. (2015, JpGU Meeting)] and our observation network clearly detected the corresponding signals. The characteristics of the detected signal are as follows: (1) the signal is dominant in the frequency range between 0.06 and 0.125 Hz, (2) the signal is particularly dominant in the vertical component, (3) the signal behaves much like Rayleigh wave, and (4) the signal propagates with a velocity about 3.2 km/s. As seismic interferometry analysis of observed seismic noise can yield surface-wave group velocities down to 0.2 Hz at the lowest due to small station-to-station distances (Hayashida et al., 2015, SSJ Fall Meeting), we utilize the abundant data for the volcanic signals to investigate surface-wave properties at lower frequencies and to validate deeper S-wave velocity structure around the bay. We selected 15 station pairs that have much smaller station-to-station distances compared to distances between Mt. Aso and the stations to assume plane wave-front propagation. Based on the phase differences of the band-pass filtered waveforms (vertical component) between two stations, we estimated Rayleigh-wave phase velocities in the frequency range between 0.05 and 0.12Hz at intervals of 0.001 Hz. The estimated phase velocities show dispersions and correspond well to those calculated from the existing crustal velocity structure model (Nishida et al., 2008, JGR) in the frequency range between 0.06 and 0.08 Hz (3.4-3.6 km/s) for most station pairs. On the other hand, at around 0.1 Hz, the estimated phase velocities show spatial variations reflecting complicated sedimentary structure beneath the area.

### Acknowledgements:

This work has been done under the Comprehensive Research on the Beppu-Haneyama Fault Zone (FY2014-2016) by the Ministry of Education, Culture, Sports, Science and Technology (MEXT).

Keywords: Aso volcano, long period tremor, phase velocity, Rayleigh wave

A method for constructing seismic velocity structure model for long-period ground motion evaluation - utilization of Rayleigh-wave dispersion information -

\*Kei Masuda<sup>1</sup>, Kazuo Yoshimoto<sup>1</sup>, Shunsuke Takemura<sup>2</sup>

1.Yokohama City University, 2.National Research Institute for Earth Science and Disaster Prevention

### Introduction

For the precise evaluation of long-period ground motions in the Tokyo metropolitan area, detailed sedimentary seismic velocity structure model of the Kanto Basin should be required. Recently, Yoshimoto and Takemura (2014) reported that, in the Kanto Basin, local sedimentary S-wave velocity structure in the vertical direction is practically characterized by using a simple three-parameter function (Ravve and Koren 2006). Takemura et al. (2015) demonstrated the effectiveness of this modeling in long-period ground motion simulations. Adopting this modeling technique, we propose a method for constructing a local sedimentary seismic velocity structure model by using Rayleigh-wave dispersion information from observed long-period ground motions and microtremor surveys, and check the effectiveness of our method based on numerical experiments.

### Method for constructing sedimentary seismic velocity structure model

Suppose that the information on Rayleigh-wave phase velocity at a certain site is available from array analyses of long-period ground motions at long-period band (6-8 s) and from microtremor surveys at short-period band (1-3 s). The three-parameter function (parameters: S-wave velocity at the surface, S-wave velocity gradient in the vertical direction, and S-wave velocity increment at a sufficiently large depth) stated above could be reduced to a two-parameter function if we let the third parameter be equal to the S-wave velocity of bedrock (Yoshimoto and Takemura, 2014). Then, by adopting empirical relations among the density, P-wave velocity, and S-wave velocity, we can formulate inversion analysis of local sedimentary seismic velocity structure as a two-parameter problem, which is easily solved by using conventional grid-search technique.

### Result of numerical experiments

We conducted a set of numerical experiments of our inversion method to confirm its effectiveness for the construction of sedimentary seismic velocity structure model. Using a sedimentary structure model of the Yokohama seismic observation well (Yamamizu 2004) as the test model, we investigated how many observations of Rayleigh-wave phase velocity are required to obtain the precise inversion result. In our numerical experiments, for simplicity, we supposed that the Rayleigh-wave phase velocities were fully available at long-period band (6, 7, and 8 s) but limitedly available at short-period band (1 or 2 or 3 s). We used a software package developed by Herrmann (2013) to calculate the dispersion characteristics of Rayleigh wave.

Our numerical experiments demonstrated that when the Rayleigh-wave phase velocity at period of 1 s was available, the distribution of squared-residuals between input and calculated phase velocities showed a most localized pattern of the minimum residuals. This result indicates that, for the use of our two-parameter modeling technique, the information on Rayleigh-wave phase velocity at period of 1 s is very useful to estimate S-wave velocity at the surface. Based on our numerical experiments, we may conclude that the construction of local sedimentary seismic velocity structures for long-period ground motion evaluation could be easily carried out by our inversion method using Rayleigh-wave dispersion information from long-period ground motions and microtremor surveys. In our presentation, we will discuss the noise stability of our inversion method and its estimation errors.

Keywords: long-period ground motion, sedimentary structure, Rayleigh-wave, phase velocity

*Estimation of 3D S-wave velocity model of sedimentary layers in Kanto area, using microtremor array measurements*

\*Kaoru Jin<sup>1</sup>, Shigeki Senna<sup>1</sup>, Atsushi Wakai<sup>1</sup>, Hiroyuki Fujiwara<sup>1</sup>

1.National Research Institute for Earth Science and Disaster Prevention

We have engaged in estimation of subsurface structure models from seismic bedrocks to ground surfaces in Kanto area for the purpose of enhancing prediction accuracy of earthquake ground motions. In order to advance the subsurface structure models, microtremor surveys have been conducted at a lot of sites in Kanto plane for these several years. Senna et.al., 2015, improved the conventional subsurface structure models by using records of microtremor array and earthquake observation. In this study, in addition to the previous described data, we will report results of microtremor array surveys with ones registered in the microtremor database of NIED and so on.

Keywords: microtremor array observation, velocity structure

*Improvement of shallow subsurface structure models based on miniature and irregular array microtremor observations in Kanto Area*

\*Atsushi Wakai<sup>1</sup>, Shigeki Senna<sup>1</sup>, Kaoru Jin<sup>1</sup>, Ikuo Cho<sup>2</sup>, Hiroyuki Fujiwara<sup>1</sup>

1.National Research Institute for Earth Science and Disaster Prevention, 2.National Institute of Advanced Industrial Science and Technology

In order to estimate damage caused by strong ground motions from a mega-thrust earthquake, it is important to evaluate broadband ground-motion characteristics in wide area. To realize it, it is necessary to sophisticate subsurface structure models on which shallow and deep ones are integrated. Therefore, we have ever collected as many data as possible obtained by boring and microtremor array surveys, and then have modeled subsurface structures from seismic bedrocks to ground surfaces.

In this study, we focus on advancement of shallow subsurface S-wave velocity structures, especially around engineering bedrocks ( $V_s300\sim500\text{m/s}$  layers), in Kanto Area, including Tokyo. We have conducted miniature and irregular array observations at a great deal of sites in Kanto plane since last year. By using these observation data, 1-D and 2-D shallow subsurface velocity structures are estimated. Then, based on these models, the initial geological models are verified and modified if necessary.

Keywords: shallow subsurface structure, velocity structure, miniature array, microtremor

An examination of the relation between the distribution of microtremor  
Horizontal-to-Vertical spectral ratios and the F distribution

\*Ikuo Cho<sup>1</sup>, Takaki Iwata<sup>2</sup>

1.National Institute of Advanced Industrial Science and Technology, 2.Tokiwa University

The distributions of microtremor Horizontal-to-Vertical Spectral Ratios (HVSr) have been investigated, with a special attention to the relation with the F distribution, on the basis of three types of microtremor waves: simple stationary waves numerically calculated with random phases, realistic waves numerically simulated based on an elastic theory and a subsurface velocity structure, and observed microtremor waves. The statistics D of the Kolmogorov-Smirnov (KS) test is used as a measure of the discrepancy between the distributions. Our simulations estimating HVSr of stationary waves with random phases indicated that the larger the circular variance of the propagating directions of microtremor waves becomes, the more a distribution of HVSr approaches the F distribution. Thus, the degree of the discrepancy from the F distribution depends on a microtremor wavefield. The analyses of realistic-simulated waves and observed microtremor waves revealed that the realizations of D took values between 1.5 and 6 % when the sample size was 3000. Since a critical value of the test lied in this range, the results of the KS test could be changed by incidental scattering. The above results indicate that the lower limit of D can be a several percent or less when the sample size is adequately large, and that a concrete value of D, as well as the results of the goodness of fit test, can depend on either biases or fluctuations in the propagating directions of microtremor waves.

Keywords: microtremor, H/V, probability distribution

## Microtremor array survey with spatial autocorrelation technique of Kazo lowland in Saitama prefecture, Japan

\*Hidetaka Shiraishi<sup>1</sup>, Shoichi Hachinohe<sup>1</sup>, Kouki Sasaka<sup>1</sup>

1.Center for Environmental Science in Saitama

We have conducted microtremor array survey with spatial autocorrelation (SPAC) techniques to estimate deep S-wave velocity structures up to 3,000 meters depth of Kazo lowland in the northeast of Saitama prefecture.

Three types of SPAC arrays, each of radii is 100m, 300m and 600m, have been deployed on the ground surface at observation sites and we have conducted microtremor observations during about one hour. Eleven sites in total have been spread out over region of approximately east-west 20km by north-south 15km. Phase velocity dispersion curves of fundamental-mode Rayleigh waves about 0.2 Hz to 1.5 Hz have been acquired.

S-wave velocity structures have been estimated through inversion analysis of dispersion curves with genetic algorithm (GA) and initial structure models have been diverted from models that had been made for an earthquake disaster prevention plan.

We have estimated one dimensional S-wave velocity structures for all of eleven sites and have made comparison the results with existing explorations. The results are generally consistent, details are however assumed that require minor modification of existing models.

Keywords: Microtremor survey method, Spatial autocorrelation technique, S-wave velocity structure

Microtremor chain array survey across the abnormal damaged zone of the 1946 Nankai Earthquake in the northern part of the Izumo Plain, Taisha-cho, Izumo City, Shimane Prefecture, Japan.

\*Hiroki Hayashi<sup>1</sup>, Yohei Kuwada<sup>1</sup>, Fawu Wang<sup>1</sup>

1. Interdisciplinary Graduate School of Science and Engineering, Shimane University

An abnormal severe damaged zone of the 1946 Nankai Earthquake was observed along the northern edge of the Izumo Plain, Taisha-cho, Izumo City, Shimane Prefecture. In this study, we carried out a microtremor chain array survey across the damaged zone for imaging the detailed surface profile of the damaged zone. Correlating with previous geologic data by using pseudo-S-wave velocity and  $N$  value, the phase velocity profile of the present survey demonstrates a buried terrace at approximately 11 meter deep as an unconformity between Pleistocene and Holocene deposits. At the center of the survey line, a buried fossil valley cutting the buried terrace was clearly recognized. It implies that the severe damage of the earthquake might be affected by the thickened soft sediments at the buried fossil valley.

Keywords: microtremor chain array, the 1946 Nankai Earthquake, Izumo Plain

## Estimation of Bogota (Colombia) basin velocity model from microtremors array measurements for strong motion simulations

\*Nelson Pulido<sup>1</sup>, Shigeki Senna<sup>1</sup>, Toru Sekiguchi<sup>2</sup>, Hiroaki Yamanaka<sup>3</sup>, Kosuke Chimoto<sup>3</sup>, Hiroto Nakagawa<sup>4</sup>, Jaime Eraso<sup>5</sup>, Helber Garcia<sup>5</sup>, Nelson Perico<sup>6</sup>, Juan Carlos Reyes<sup>7</sup>

1.National Research Institute for Earth Science and Disaster Prevention, 2.Chiba University, 3.Tokyo Institute of Technology, 4.Building Research Institute, 5.Servicio Geológico Colombiano, 6.Instituto Distrital de Gestión de Riesgos y Cambio Climático, 7.Universidad de los Andes

Bogota a megacity with almost 8 million inhabitants is prone to a significant earthquake hazard due to nearby active faults as well as subduction megathrust earthquakes. The city has been severely affected by many historical earthquakes in the last 500 years, reaching MM intensities of 8 or more in Bogota. The city is also located at a large lacustrine basin composed of extremely soft soils which may strongly amplify the ground shaking from earthquakes. The basin extends approximately 40 km from North to South, is bounded by the Andes range to the East and South, and sharply deepens towards the West of Bogota. The city has been the subject of multiple microzonations studies which have contributed to gain a good knowledge on the geotechnical zonation of the city and tectonic setting of the region. In order to construct a detailed velocity model of the basin we conducted 68 small to medium size microtremors arrays measurements (radius from 60 cm to 50 m) at 26 sites within the city, and two large arrays measurements at the central part of the basin (radius of 500 m and 1000 m). We calculated dispersion curves and inferred velocity profiles at all the sites. Our velocity profiles for the shallower sediments are characterized by a wide variability in  $V_{s30}$  whose values range from 80 ~ 150 m/s in the northern and central part of the basin, and 120 ~390 m/s in the southern part. Our velocity models reached values of  $V_s=2000$  m/s at a 2 km depth at the central part of the basin, but previous models suggest that the basin depth may largely increase further west. Our preliminar results indicate a sharp boundary in shallow S wave velocities between very soft sediments North of the basin and harder sediments to the South. This striking difference appears to have a strong correlation with the very large water content of the shallower soils (clays and silts) to the North as compared to the small water content of soils (gravels and sands) to the South. Our initial results indicate the need of denser microtremors measurements within the city by including large arrays that allow to characterize in detail the geometry of the basin depth.

### Acknowledgements

These activities are a component of a multidisciplinary cooperative research project between Colombia and Japan entitled "Application of state of the art technologies to strengthen research and response to seismic, volcanic and tsunami events and enhance risk management in Colombia (2015-2019)", sponsored by SATREPS. We would like to thank members of our SATREPS team involved in this study; Monica Arcila, Diana Arevalo, Ivan Bautista, Luisa Castillo, Cristina Dimaté, Cristian Gonzalez, Jessica Luengas, Elizabeth Mayo, John Mora, Patricia Pedraza, Leonardo Quiñones, Gustavo Redondo, Andrea Riaño, Marta Tovar.

Keywords: Soil velocity model, Strong motion simlation, Bogota basin

## The strong resemblance between Fourier Spectrum and Phase difference Spectrum of the Seismic Wave.(Science of Form)

\*Masaru Nishizawa<sup>1</sup>

1.none

1.The phase difference Spectrum and The Phase Wave of the seismic wave.

Fig-(1). Show "The relationship between the phase difference spectrum and the phase wave". Please refer to reference (3). Find the phase difference Spectrum from the phase wave on the right -hand side, the peak position and added an expanse state of Spectrum are in perfect harmony accord. In short (in other words), in case of the frequency of the phase wave is high, the shape of the normal distribution of the phase difference spectrum is build up sharp. And in the case of large frequency get a flat normal distribution of spectrum. This phenomena stand up all right frequency is high or low. Of course this phenomena is reversible was stated reference (3).

I shall state a next item 2, the seismic wave and this phase wave should be a one-to-one relation. And still more the Fourier spectrum of the seismic wave and the phase difference Spectrum should be a one-to-one relation.

2.The Fourier Spectrum and the normal distribution of seismic wave.

We think that the case of the epicenter length is becoming shorter little by little. The large epicenter length to get along with, the seismic wave energy is dispersed in every direction and still more had died out. As a result, the shape of the Fourier spectrum don't become a hill shape and happened occasionally a pointed shape. The shorter epicenter length to get along with, the shape of the Fourier spectrum of seismic wave is formed a hill and soon are considered the shape of the normal distribution.

Reference. "Earthquake" written by Seismologist KIYOO Wadachi. The Chuukou Library. (A pocket edition) 1933 and 1993(reprint) p.99

"In the near area to the epicenter, the earthquake have very sharp motion. In many case, intense vertical motion happens in the early shocks of an earthquake. The longer the epicenter length little by little, vibration of seismic wave become slow little by little and becomes superior in a horizontal vibration."

The shape of this normal distribution has flat hill and besides has large frequency of the peak of the hill. But get shorter little by little, the shape of the normal distribution (or Bell type) becomes sharp and becomes short frequency.

Moreover make the short epicenter length, we shall study the normal distribution theory (Gaussian distribution, Mt.Fuji-type or Bell type) of probability and statics.

In the reference (4), I have explained the KdV equation.(literature (3),(4))

Abstract

1. The shorter epicenter length shorter, the shape of the normal distribution becomes sharp. And this frequency too becomes small. The case of the epicenter length is large, the normal distribution of spectrum of seismic wave was not build up. Only build up a scattered peak.

2. On the case of the phase wave and the phase difference spectrum, the same phenomenon too come into being.

Reference

1. Yorihiro Osaki "Shin Jishindou no Spectrum Kaiseki Nyumon" P78.

2. Masaru NISHIZAWA. (2012): Study of shape of Mountain (Normal Distribution) of Fourier Spectrum of Earthquake Motion. May 20-25, S-SS30-P12(2012, JpGU)

3. Masaru NISHIZAWA. (2012): Handling by Solitary Wave and soliton of Earthquake Motion: October

D22-01, 2012, The Seismological Society of Japan.

4. Masaru NISHIZAWA. (2015): Normal Distribution of Seismic Wave Spectrum and Solitary Wave in Water Waves (Science of Form). October 27. S01-P20, 2015, The Seismological Society of Japan.

5. Research Report on the 2011 Great East Japan Earthquake Disaster. NIED, Japan.

Keywords: Fourier Spectrum, Phase difference spectrum, Seismic wave, Phase wave, KdV equation, Solitary wave

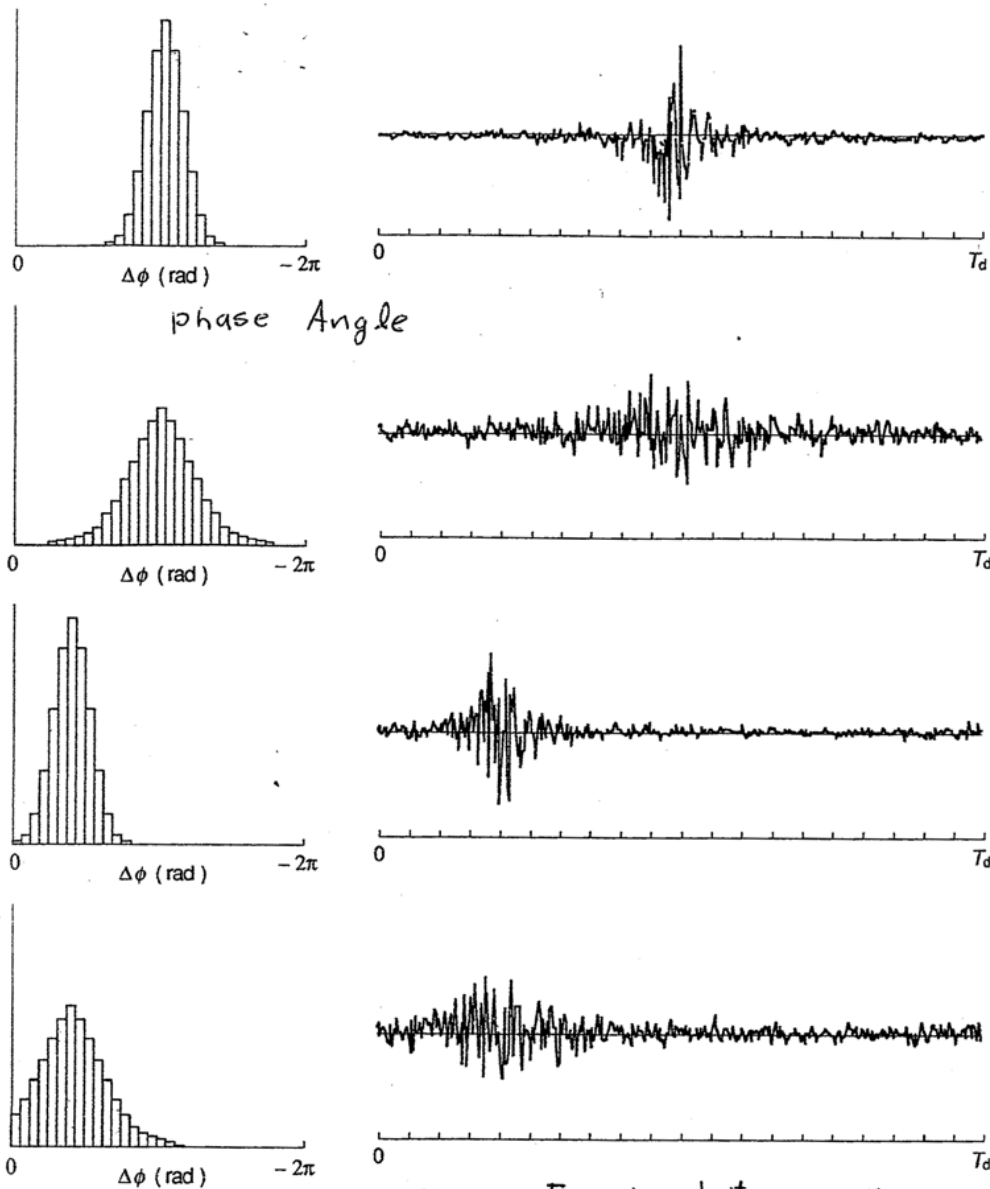


Fig-1 The relationship between the phase difference spectrum and the phase wave.  
~~図-1~~ 位相差分スペクトルと位相波の関係